Effects of hypoxia on the heart of the juvenile four-finger threadfin (*Eleutheronema tetradactylum*) based on physiological indicators and transcriptome analysis

Yi Lu[1], Eric Amenyogbe[2], Ye- Yang[1], Zhong-liang Wang[1,3,4],
Jing-hui Jin[1], Rui-tao Xie[5], Eric Kwabena Droepenu[2]
and Jian-sheng Huang[1,3,4]*

[1]Fishery College, Guangdong Ocean University, Zhanjiang, China, [2]Department of Water Resources
and Aquaculture Management, University of Environment and Sustainable Development, Somanya,
Eastern Region, Ghana, [3]Guangdong Provincial Key Laboratory of Aquatic Animal Disease Control and
Healthy Culture, Zhanjiang, China, [4]Guangdong Marine Fish Science and Technology Innovation
Center, Zhanjiang, China, [5]Guangdong Evergreen Feed Industry Co. Ltd, Zhanjiang, China

This study evaluated the effects of hypoxia on the heart of juvenile four-finger threadfin (*Eleutheronema tetradactylum*) through physiological and transcriptome analysis. Juveniles with an average weight of 122.82 g and length of 24.60 cm were used. Hypoxia significantly increased serum myocardial enzyme activities, including creatine kinase (CK), creatine kinase-MB isoenzyme, lactate dehydrogenase (LDH), and α-hydroxybutyrate dehydrogenase (HDBH). These indicators initially rose and then declined, reflecting cardiac stress and suggesting their potential as early hypoxia biomarkers for real-time aquaculture monitoring. Histological analysis revealed structural damage in myocardial fibers under hypoxia, with increasing severity over time. This underscores the need to minimize oxygen fluctuations to prevent cardiac tissue degeneration. Transcriptome analysis identified upregulated genes involved in cell communication, immune responses, and intracellular signaling, offering potential targets for breeding hypoxia-tolerant species. Kyoto Encyclopedia of Genes and Genomes pathway enrichment analysis highlighted key pathways such as mitogen-activated protein kinase (MAPK), hypoxia-inducible factor-1 (HIF-1), endocytosis, and phagosome formation. The MAPK pathway plays a critical role in cellular stress responses, including survival, proliferation, and apoptosis. Hypoxia-induced activation of MAPKs like ERK, JNK, and p38 regulates stress-responsive genes. HIF-1 signaling regulates oxygen homeostasis, with HIF-1α stabilizing hypoxia-responsive genes such as VEGFA, which promotes vascular remodeling and enhances oxygen delivery. These findings collectively offer practical applications for enhancing aquaculture management, such as monitoring biochemical markers, adopting hypoxia-

tolerant breeding, and adjusting environmental conditions to mitigate stress, ensuring better productivity and sustainability. This research provides a foundation for further studies on the molecular mechanisms of hypoxia stress in aquaculture species.

1 Introduction

The four-finger threadfin (*Eleutheronema tetradactylum*) holds substantial aquaculture value, especially in coastal regions in Asia where it is cultivated for its economic potential (Soe et al., 2023; Xuan and Wang, 2023). However, due to intensive aquaculture practices, hypoxic conditions frequently arise, posing a significant threat to its survival and growth. Hypoxia affects several vital physiological processes in *E. tetradactylum*, with a particularly adverse impact on the heart (Gu et al., 2023), which is crucial for oxygen transport and metabolic regulation (Xuan and Wang, 2023; Iqbal et al., 2023; Wang et al., 2023; Li et al., 2022). The heart is particularly vulnerable to hypoxia due to its high metabolic demand and reliance on aerobic metabolism to sustain contractile function. Unlike some other organs, which can temporarily switch to anaerobic pathways for energy production, the heart's dependence on oxygen for ATP synthesis is critical for maintaining its continuous pumping action (Cerra et al., 2023; Doenst et al., 2013; Essop, 2007; Ošťádal and Kolář, 1999). This makes it highly susceptible to reduced oxygen levels. Prolonged exposure to low oxygen levels disrupts myocardial enzyme activity, damages cardiac tissue, and triggers a series of gene expression changes (Yohana et al., 2024; San et al., 2021; Jiang et al., 2021; Chen et al., 2021, 2017).

Dissolved oxygen is a key environmental factor affecting fish growth, metabolism, and survival (Wang et al., 2023; Ali et al., 2022). Hypoxia, generally defined as dissolved oxygen concentrations below 3 mg/L, impacts multiple physiological processes in fish, including growth, reproduction, and metabolic regulation (Yohana et al., 2024; San et al., 2021; Jiang et al., 2021; Chen et al., 2021, 2017). Different species and even tissues within the same organism exhibit varying levels of oxygen tolerance. In *E. tetradactylum*, hypoxia predominantly affects the gills, liver, and intestines, resulting in changes in physiological and biochemical activities, enzyme function, gene expression, and signaling pathways, such as the hypoxia-inducible factor-1 (HIF-1) pathway (Liu et al., 2024; Wang et al., 2023; Gu et al., 2023; Huang et al., 2021). These processes underscore the complexity of the physiological responses to oxygen deprivation and highlight the importance of studying the molecular mechanisms underlying hypoxia tolerance.

Despite fish having well-documented capacities to survive low oxygen conditions, research on the molecular regulatory mechanisms of their response to hypoxia is still developing. Understanding how fish respond to hypoxic stress at a physiological and molecular level is crucial for breeding programs aimed at enhancing hypoxia tolerance in aquaculture species. Juvenile fish, in particular, are more vulnerable to environmental stressors like hypoxia, which can significantly affect their growth and survival (Canosa and Bertucci, 2023). Studying the responses of juvenile *E. tetradactylum* to hypoxia will help improve aquaculture practices and management strategies.

The heart, being central to oxygen transport and metabolic regulation, plays a critical role in the hypoxic response of fish (Zhao et al., 2023). Physiological indicators such as heart rate, cardiac output, and oxygen consumption provide valuable insights into how hypoxia affects cardiac function (Galli et al., 2023). Studies have shown that acute hypoxia may lead to the preferential perfusion of vital organs like the heart, temporarily maintaining cardiac function. However, sustained hypoxia can impair myocardial contractility, reduce cardiac output, and potentially lead to heart failure (Everett et al., 2012). Investigating the mechanisms by which the heart adapts to hypoxic stress is, therefore, essential to understanding the overall resilience of *E. tetradactylum* to environmental challenges.

Transcriptome sequencing is a powerful tool for studying gene expression and regulation at the molecular level. It has been extensively used to investigate stress responses, metabolic regulation, and the genetic basis of various physiological processes in fish. Transcriptome analysis offers a detailed understanding of the molecular mechanisms underlying physiological changes in response to environmental stressors, including hypoxia (Sun et al., 2021). In recent years, genes and signaling pathways related to hypoxia stress have been identified in several fish species, such as cobia (*Rachycentron candum*) (Huang et al., 2023), bighead carp (*Hypophthalmichthys nobilis*) (Chen et al., 2021), and large yellow croaker (*Larimichthys crocea*) (Mu et al., 2020). However, hypoxia response mechanisms are species-specific, underscoring the need for species-focused research.

The study integrates physiological indicators with transcriptomic profiling, enabling a multi-faceted approach to assess hypoxia's impact on cardiovascular function, which provides a deeper understanding of metabolic, structural, and genetic adaptations. Specifically, it identifies unique hypoxia-responsive genes linked to energy efficiency and

reduced oxidative stress, supporting the resilience of the heart under low-oxygen conditions. This dual analysis approach, combining physiological changes with molecular insights, offers a comprehensive view of hypoxia-induced cardiac adaptations, facilitating the development of strategies for hypoxia-tolerant aquaculture species.These insights are critical for the conservation and sustainable management of *E. tetradactylum* populations and contribute to the broader understanding of hypoxia's impact on marine fish species. The findings also provide a theoretical basis for breeding new hypoxia-resistant strains and serve as a reference for improving the health and cultivation practices of four-finger threadfin in aquaculture systems.

2 Materials and methods

2.1 Experimental fish and feeding management

The experimental fish were derived from juveniles bred in the biological research base of Donghai Island, China, by the fish seed engineering and breeding team of the Fisheries College of Guangdong Ocean University. Five hundred healthy individuals with an average weight of 122.82g and average length of 24.60cm were randomly selected and transported to the Guangdong Evergreen Feed Industry Co., Ltd., breeding base, Zhanjiang, China, with a special fry transport vehicle. The breeding facility is an indoor 1000 mL breeding tank with a 24-hour continuous inflatable microwater aquaculture system. As feeding water, natural seawater was used that had undergone sedimentation and sand filtration to ensure that the experimental water meets the national fishery water quality standard (GB 11607-89). Throughout the experiment, several critical water quality parameters were meticulously monitored and controlled to ensure consistency. These parameters included pH, temperature, dissolved oxygen, ammonia, and salinity. A multiparameter apparatus (HI 9828, Hanna Instruments, Keison Co., Chelmsford, UK) was utilized to maintain these parameters at stable levels, thereby enhancing the reliability of the experimental outcomes (Noureen et al., 2023). During the temporary maintenance period, the dissolved oxygen (DO) level was ≥ 5 mg/L, ammonia nitrogen was 0.10 ± 0.03 mg/L, pH was 8.1, water temperature was 28 ± 0.5°C, and salinity was 28–30. At both 8:00 and 17:00 every day, feed with special formula was given once (Guangdong Evergreen Feed Industry Co., Ltd., crude protein content ≥ 55%, crude fat content ≥ 8%, crude fiber content ≤ 3%, and crude ash content ≤ 16%). One hour after the start of the feeding, fish feces and residual feed were removed. The experiment started after two weeks of acclimatization.

2.2 Experimental design and sample collection

At the end of the holding period, fish were fasted for 24 h and randomly divided into two treatment groups: a hypoxic stress group (DO: 3.1 ± 0.26 mg/L) and a control group (CG; DO: 5.74 ± 0.23

mg/L), with three replicates per group and 20 fish per replicate. The tanks of CG were continuously aerated and circulated with water. A DO meter (AZ8403, Hengxin, Taiwan) was used to monitor the changes in DO every 10 min. In the hypoxic group, DO levels were adjusted by controlling the flow of circulating water, closing the inflow, and covering the water tank with a membrane from above; a DO meter (AZ8403, Hengxin, Taiwan) was used for real-time monitoring (Wang et al., 2021; Xie et al., 2021; Zhang et al., 2021).

All experimental processes were performed in accordance with the regulations for laboratory animals of Guangdong province, China. This study was conducted in compliance with the guide of the Guangdong Ocean University Research Council for the care and use of laboratory animals. Five juveniles were randomly sampled from CG and hypoxic group on days 1, 4, and 7. Fish were euthanized using ethyl-3-aminobenzoate methanesulfonate (MS-222, Sigma, USA) to facilitate blood and heart tissue collection. After their collection, hearts of fish were frozen in liquid nitrogen and quickly moved to -80°C until further studies. The sampling time of experimental group and CG was the same. The group exposed to hypoxia stress for 1 day was named HG-1d, that exposed to hypoxia stress for 4 days was named HG-4d, and the group exposed to hypoxia stress for 7 days was named HG-7d.

2.3 Measurement of myocardial enzyme activity

Creatine kinase (CK), creatine kinase myocardial band isoenzyme (CK-MB), lactate dehydrogenase (LDH), and α-hydroxybutyrate dehydrogenase (HBDH) were determined in heart tissues of juvenile fish by relevant test kits (Nanjing Jiancheng Technology Co., Ltd., http://www.njjcbio.com/). The steps are briefly described as follows: Cryopreserved heart tissue was thawed and weighed accurately; then, nine times normal saline was added according to the ratio of weight (g): volume (mL) = 1:9. The frozen heart tissue was homogenized in an ice water bath for 3–5 min, and then centrifuged at 4°C and 2,500 r/min for 10 min. According to the instructions of the relevant kit, the supernatant was used to determine CK, CK-MB, LDH, and HBDH levels. CK-MB was determined by immunosuppression, CK and LDH were determined colorimetrically, and HBDH was determined by the α-ketobutyrate substrate method.

2.4 Fabrication and observation of heart tissue microsections

The paraformaldehyde-fixed heart was rinsed with water, dehydrated with a 70–95% ethanol gradient, and transparented with xylene. After paraffin embedding, the heart was continuously sectioned (Leica microtome RM2016, Leica, Shanghai, China) to a thickness of 5–6 μm. Hematoxylin and eosin staining and neutral resin mounting were used to observe sections and photos were taken under an optical microscope (Nikon E80i microscope with Nikon Y-TV55 imaging system, Nikon, tochigi, Japan).

2.5 RNA extraction, cDNA library construction, and raw sequencing data acquisition

Heart tissue samples of three fish from each of the hypoxia stress group (HG-7d) and CG were removed from -80°C refrigeration, ground to powder by adding liquid nitrogen in a pre-cooled mortar, and total RNA was extracted using TRIzol reagent (Invitrogen, Waltham, MA, USA) according to the manufacturer's instructions. The purity of RNA was tested using a Nanodrop2000 spectrophotometer (Thermo Fisher Scientific, Waltham, MA, USA). Agarose gel electrophoresis was used to detect RNA integrity, and an Agilent2100 was used to determine the RNA integrity number. mRNA was purified from total RNA using Oligo(dT)-labeled magnetic beads. Fragmentation was performed using divalent cations at high temperature in NEBNext first-strand synthesis reaction buffer (5×). First-strand cDNA was synthesized using random hexamer primers, followed by second-strand cDNA. To select cDNA fragments with a length of 240 bp, library fragments were purified using the AMPure XP system (Beckman Coulter, Brea, CA, USA) and then PCR amplified. After the library quality inspection had passed, the cDNA library was sequenced using the Illumina HiSeq high-throughput sequencing platform. To eliminate individual differences according to the method of mixing tissue samples by Liu et al. (2013), in this experiment, heart tissue samples of three fish per group were mixed in equal amounts. Then, 1 μg of RNA from each group was used for cDNA library construction and Illumina sequencing. The library construction and Illumina sequencing in this study were completed by Genedenovo Co., Ltd. (Guangzhou, China). As reagents used for library construction, the Truseq TM RNA sample prep Kit (Illumina, CA, USA) was used and the sequencing system was Illumina Novaseq 6000 (Illumina, San Diego, USA), with the sequencing mode 2 × 150 bp.

2.6 Data processing, assembly, and functional annotation

The raw data obtained by sequencing were obtained by removing sequencing adapters and primer sequences from the reads and filtering low-quality data to obtain clean data, which were then assembled from scratch using Trinity (v2.5.1). Longer transcript sequences were obtained by overlapping splicing, and the longest transcript in the same gene was selected as unigene. The transcripts obtained after de-redundancy of the assembled transcripts were annotated. The obtained assembled transcripts were compared with the non-redundant protein (NR), Kyoto Encyclopedia of Genes and Genomes Orthology (KEGG), and Swiss-Prot databases using the Diamond program. The obtained assembled transcripts were compared with the clusters of orthologous groups for complete eukaryotic genomes database by NCBI blast v2.2.29+, and the transcripts were annotated.

2.7 DEG analysis, GO enrichment, and KEGG enrichment

Bowtie was used to align the reads obtained by sequencing with the unigene library. The expression level was estimated based on the alignment results combined with RSEM. The fragments per kilobase of transcript per million fragments mapped value was used to represent the expression abundance of the corresponding unigene. DESeq2 was used to perform differential expression analysis between sample groups to obtain the differentially expressed gene (DEG) set between two conditions. The Benjamini–Hochberg method was used to correct the significance obtained by the original hypothesis test; further, the P value was also corrected, i.e., FDR < 0.01 and log2FC obtained by the original sample groups, to obtain the DEG set between the two conditions; various annotation information corresponding to DEGs was obtained.

2.8 Real-time fluorescence quantitative PCR verification

Ten DEGs (five of which were upregulated and five were downregulated) were randomly selected from the sequencing results. Primers were designed using Primer premier 5 software (Table 1) using *Rps4* as the internal reference for quantitative real-time PCR (qRT-PCR) verification. The reaction procedure was performed in three steps: pre-denaturation at 94°C for 30 s, and 40 cycles including denaturation at 94°C for 5 s, annealing at 60°C for 15 s, and extension at 72°C for 20 s. Each sample was tested three times, and the results were calculated by the $2^{-\triangle\triangle Ct}$ method (Song et al., 2020; Rao et al., 2013). Finally, the results were drawn according to the data of the relative expression levels between samples and CG.

TABLE 1 Primer sequences of genes used for quantitative real-time PCR.

Genes	Primer sequences(5′–3′)
ldha	GTCATCGGCTCTGGCACCAA, CCTCCTTCCACTTCTCGCTGTC
PTGS2	ACAGTCTGGAGAGGCAACACAA, AGCGAAGCGGTGAGAGTCTG
jak1	CGTGAAGGAGTCTCGTGCTGTT, GCTGGAAGTGGAGGTTGTCTGT
cfl1-a	AGCGGTTGCGATTGGTGGTA, TGGCAGTCATACAGCAGGTAGC
KSR1	GACAACCGCTTCCACTTC, CTCGTCACACTCCTCAGA
CNDP2	CCTCCGTCCTGCTGCTCATT, CCTGTTCTCCGATGTCCACCA
lipt2	ATGGTTTGACCACATCGTGC, CGTTGTCCTCGTCACCTCC
IP6K2	CAGGCTGAGGTGCTCTACTACA, GCTTGGCGTTCTCCTTCATCC
tmem205	GGAGCCGACAGACTTCATCAA, AGTTACCTGCTTCACCAACACA
unc45b	GTGTGCCTCTGCTGCTCAAC, TGCCAGTGCGATCTCTTCATTG
Rps4	GGCGAGCACTTCCGTCTGAT, CGGTGTCGTTGACCTTGATGAG

2.9 Data analysis

Graphpad prism 10 software was used to process and map the data. Paired t-tests were used to analyze differences between CG and hypoxia stress groups. The difference was considered significant at $P < 0.05$, and extremely significant at $P < 0.01$. Statistical methods used to verify the significance of cardiac enzyme activity: All values are expressed as mean ± standard error (M ± SE). Statistical analysis was performed using Prism 10 software. The hypoxia group and the control group were compared using t test. $P < 0.05$ was considered a significant difference, and $P < 0.01$ was considered an extremely significant difference.

3 Results

3.1 Effects of hypoxia on myocardial enzyme activities in the four-finger threadfin

The effect of hypoxia stress on myocardial enzyme activities in the four-finger threadfin is shown in Figure 1. Hypoxia caused significant fluctuations in myocardial enzyme activities which initially increased, then stabilized or returned to baseline, suggesting a biphasic response involving initial stress and subsequent adaptation.With the extension of hypoxia stress time, the activities of CK, LDH, and HDBH first increased and then decreased. The activity of CK-MB followed a significant increasing trend. Among them, CK activity and HDBH activity reached peak values after 4 days of hypoxia stress, and were significantly higher than those in CG ($P < 0.01$); moreover, LDH activity was also significantly higher than in CG ($P < 0.05$). After 7 days of hypoxia stress, CK activity and LDH activity returned to the level of CG ($P > 0.05$), while CK-MB activity and HDBH activity were still significantly higher than those of CG ($P < 0.01$).

3.2 Effects of hypoxia on the cardiac tissue structure of the four-finger threadfin

The effect of hypoxia on the cardiac tissue structure of the four-finger threadfin is shown in Figure 2. Prolonged hypoxia exposure led to progressive structural damage in cardiac tissue, marked by increased cell gaps, disordered fibers, and cell swelling, indicating that sustained hypoxia can severely impair heart tissue integrity. The myocardial fibers of the fish of CG were continuously and neatly distributed, and myocardial cells were arranged in longitudinal, oblique, and circular bundles without expansion or breakage (Figure 2A). However, the degree of structural damage of the cardiac tissue in the hypoxia group increased gradually with the extension of time under stress. This damage manifested as the gradual enlargement of the intercellular gaps in the myocardium, and the disorder, swelling, and even rupture of muscle fibers (Figures 2B–D).
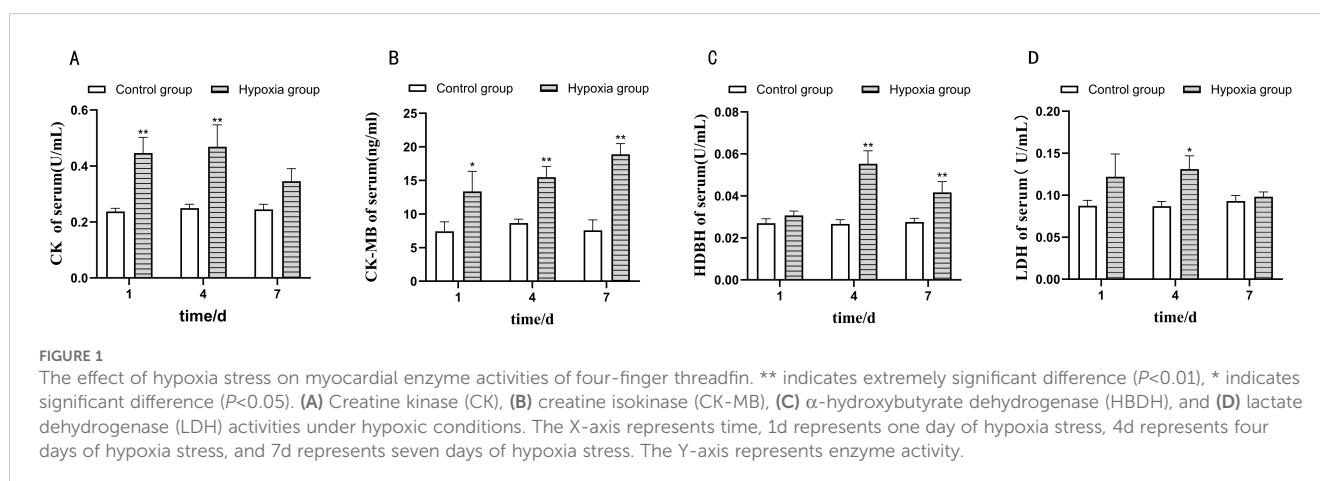
3.3 Transcriptome analysis

3.3.1 Results of transcriptome sequencing data quality assessment

Transcriptome analysis identified several differentially expressed genes (DEGs), showing a strong initial upregulation, a modulation phase at four days, and then increased gene activation at seven days. These DEGs were associated with immune responses, oxidative stress management, and cell communication, pointing to adaptive mechanisms aimed at maintaining heart function under low oxygen conditions.The base distribution and sequencing quality of the quality control sequences of 12 samples were obtained. The GC content was 47.86–49.21%, Q20 (sequencing accuracy 99%) was 97.21–97.72%, and Q30 (sequencing accuracy 99.9%) was 92.43–93.63%, which can be used for subsequent analysis and research. The results of the comparison are presented in Table 2.

3.3.2 DEG screening results

Differentially Expressed Genes (DEGs), these are genes that show a significant difference in expression levels (upregulation or downregulation) between experimental conditions, such as hypoxia and normal oxygen levels. Identifying DEGs helps reveal genes associated with stress responses and adaptations. DEGs were screened in three comparison groups: CG *vs* HG-1d group, CG *vs* HG-4d group, and CG *vs* HG-7d group. The results are shown in Figure 3. A total of 729 DEGs were screened in the CG *vs* HG-1d group, 674 of which were upregulated and 55 were downregulated.

FIGURE 1
The effect of hypoxia stress on myocardial enzyme activities of four-finger threadfin. ** indicates extremely significant difference (*P*<0.01), * indicates significant difference (*P*<0.05). **(A)** Creatine kinase (CK), **(B)** creatine isokinase (CK-MB), **(C)** α-hydroxybutyrate dehydrogenase (HBDH), and **(D)** lactate dehydrogenase (LDH) activities under hypoxic conditions. The X-axis represents time, 1d represents one day of hypoxia stress, 4d represents four days of hypoxia stress, and 7d represents seven days of hypoxia stress. The Y-axis represents enzyme activity.
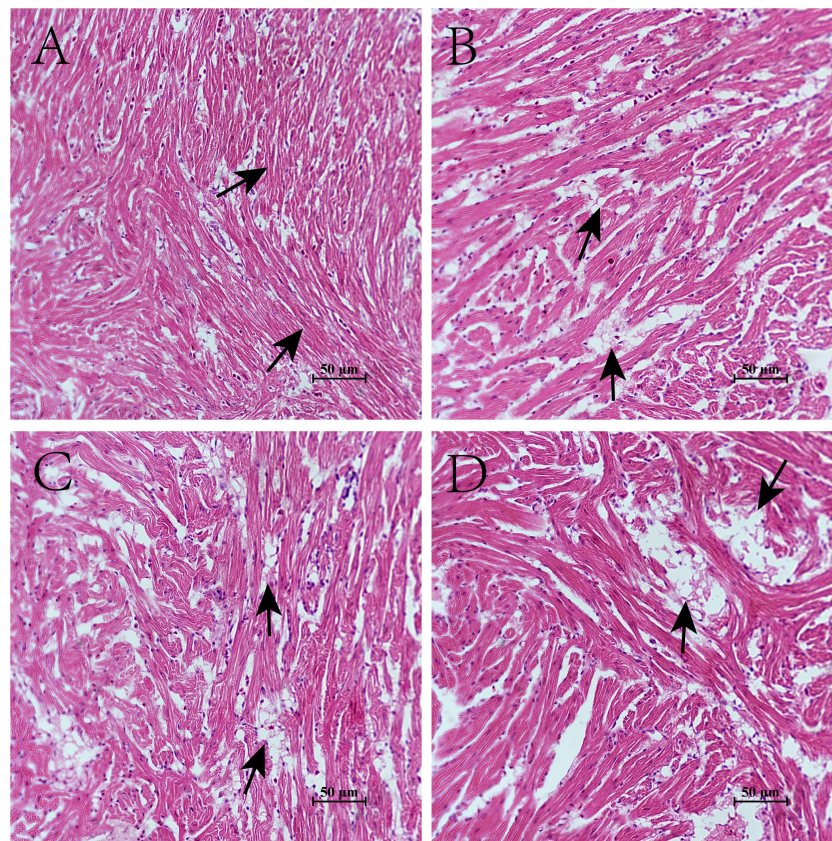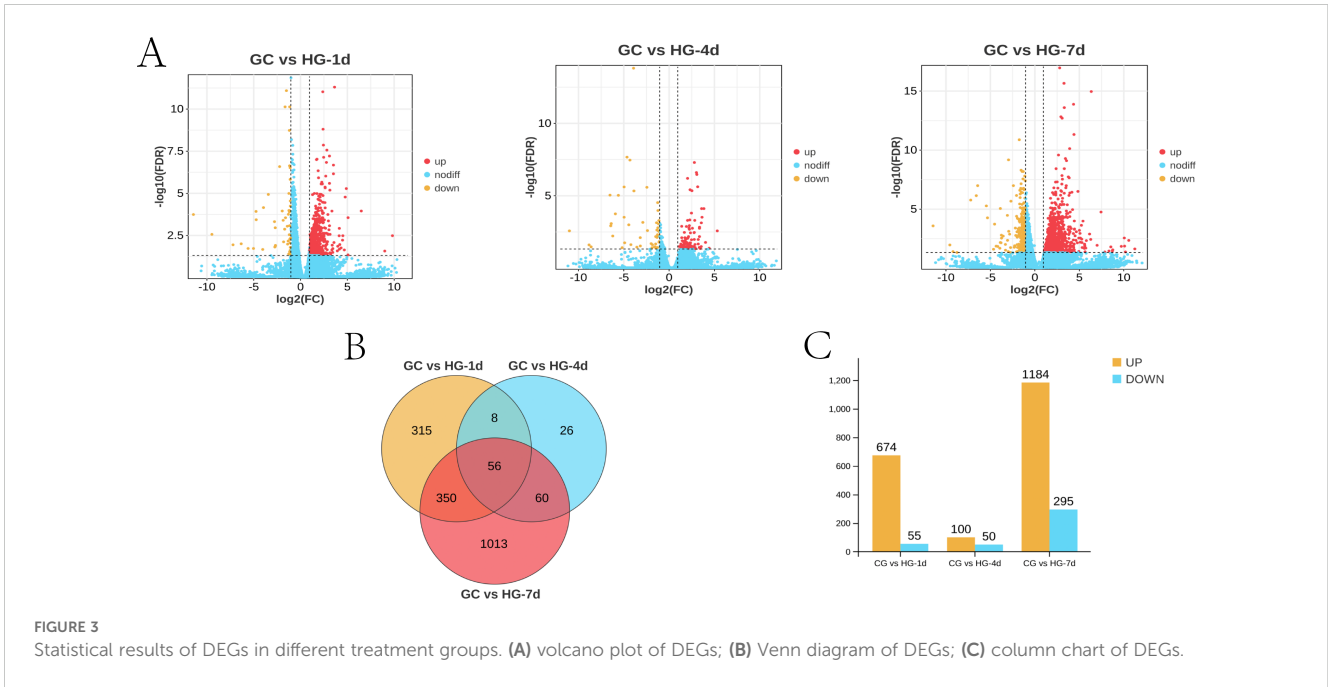
FIGURE 2
Effects of hypoxia on the cardiac tissue structure of four-finger threadfin. **(A)** control group (CG); **(B)** hypoxia stress 1d (HG-1d); **(C)** hypoxia stress 4d (HG-4d); **(D)** hypoxia stress 7d (HG-7d).

TABLE 2 Statistical comparison of the raw and clean sequencing of the RNA-seq library of heart samples of the four-finger threadfin.

Sample	Raw reads	Clean reads	Clean bases ratio (%)	Q20 (%)	Q30 (%)	GC contents (%)	Total mapped(%)
CG-1	40690034	40521192	99.59	97.63	93.40	48.37	65.45
CG-2	42880586	42701114	99.58	97.70	93.63	48.18	68.72
CG-3	39749026	39561504	99.53	97.61	93.38	49.21	68.72
HG-1d-1	39647326	39489126	99.60	97.69	93.59	48.41	71.54
HG-1d-2	47263258	47045704	99.54	97.40	92.94	48.54	71.91
HG-1d-3	45337108	45103744	99.49	97.21	92.43	47.86	66.92
HG-4d-1	37802902	37652372	99.60	97.57	93.25	48.59	70.78
HG-4d-2	38953094	38817176	99.65	97.72	93.53	48.24	66.80
HG-4d-3	38081188	37912272	99.56	97.57	93.30	48.83	68.19
HG-7d-1	39008042	38846388	99.59	97.64	93.50	48.77	73.21
HG-7d-2	38296944	38151754	99.62	97.58	93.28	49.04	74.59
HG-7d-3	41199634	41031946	99.59	97.47	93.09	48.15	66.16

Raw reads refer to unfiltered reads that have been downloaded. Clean reads refer to reads from which low-quality reads were filtered out. Raw bases refer to the total number of bases that have been downloaded (number of reads × read length). Clean bases refer to the total number of bases from which low-quality reads were filtered out. Clean reads ratio (%) refers to the ratio of reads with filtered out low-quality reads to Raw reads. Clean bases ratio (%) refers to the ratio of bases with filtered out low-quality bases to Raw bases; Q20 and Q30 refer to the percentage of bases with values greater than 20 and 30, respectively, among total bases. GC refers to the percentage of the sum of the number of calculated bases G and C to the total number of bases.
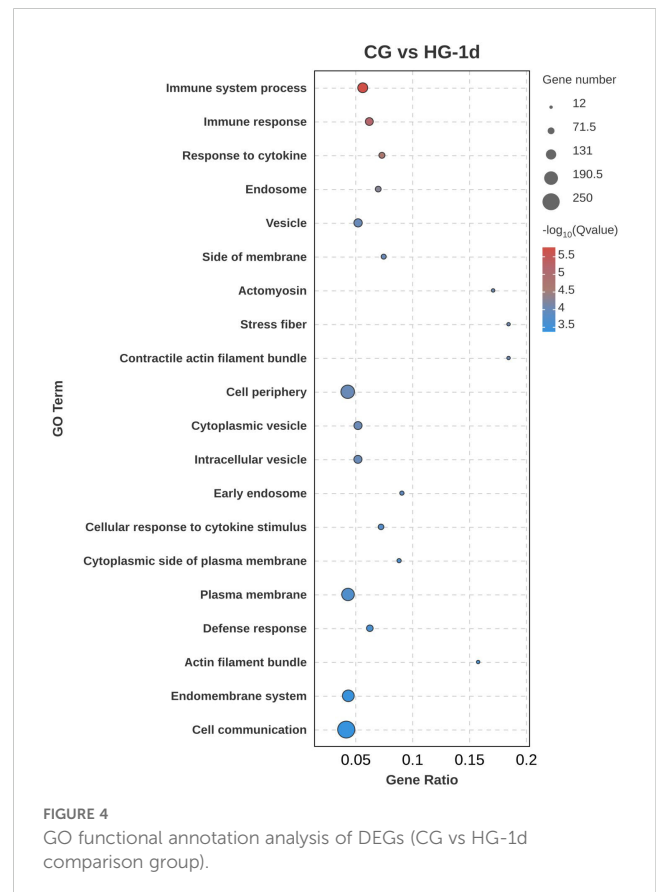
FIGURE 3
Statistical results of DEGs in different treatment groups. **(A)** volcano plot of DEGs; **(B)** Venn diagram of DEGs; **(C)** column chart of DEGs.

A total of 150 DEGs were screened in the CG *vs* HG-4d group, 100 of which were upregulated and 50 were downregulated. A total of 1,479 DEGs were screened in the CG *vs* HG-7d group, 1,184 of which were upregulated and 295 were downregulated (Figure 3).

3.3.3 GO functional annotation analysis results of DEGs

To determine the physiological regulation involved in the DEGs in the heart tissue of the four-fingered threadfin during its adaptation to hypoxia, Gene Ontology (GO) functional annotation analysis of DEGs was performed. Gene Ontology is a framework that categorizes genes and their products based on known biological processes, cellular components, and molecular functions. GO analysis enables researchers to understand the roles of DEGs in specific biological contexts, such as how genes are involved in cellular responses to hypoxia. The results showed that DEGs were distributed in biological process, cellular component, and molecular function, among which the number of DEGs enriched in cellular component was the largest. In the CG vs HG-1d group (Figure 4), the main functions were cell communication (GO: 0007154), cell periphery (GO: 0071944), and plasma membrane (GO: 0005886), with 250, 188, and 171 DEGs annotated, respectively. In the CG vs HG-4d group (Figure 5), the main functions were catalytic activity (GO: 0003824), immune system process (GO: 0002376), and oxidoreductase activity (GO: 0016491), with 70, 31, and 26 DEGs annotated, respectively. In the CG vs HG-7d group (Figure 6), the main functions were plasma membrane (GO: 0005886), intracellular signal transduction (GO: 0035556), and immune system process (GO: 0002376), with 354, 258, and 232 DEGs annotated, respectively. In addition, other functional categories, such as biological regulation (GO: 0065007), vesicle (GO: 0031982), cytoplasmic vesicle (GO: 0031410), intracellular vesicle (GO: 0097708), and cell activation (GO: 0001775) found in the heart were also significantly enriched, with 391, 209, 199, 199, and 125 DEGs, respectively. During hypoxic stress, the enrichment of DEGs in the

regulatory processes of cell membranes and immune systems was stronger. This showed that the heart tissue produced a large number of processes involved in cellular immunity and other related activities.
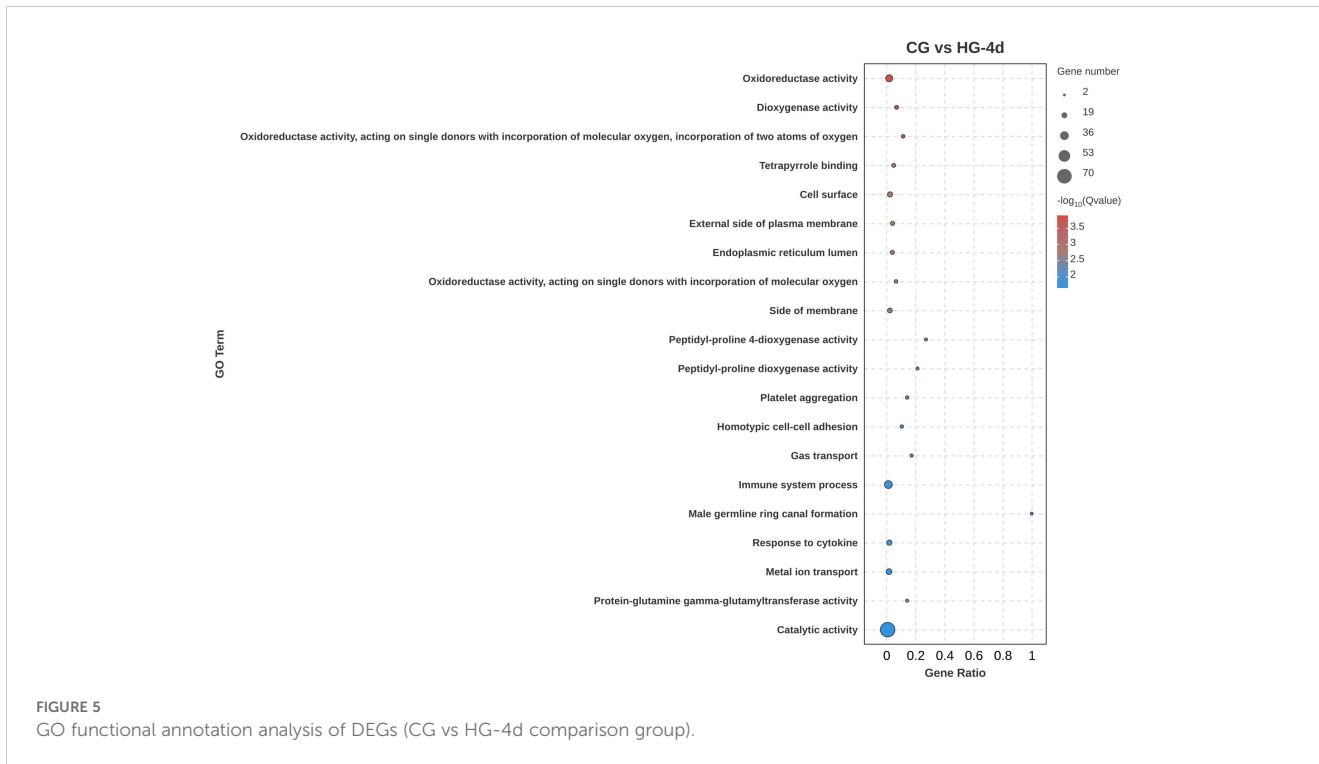

FIGURE 4
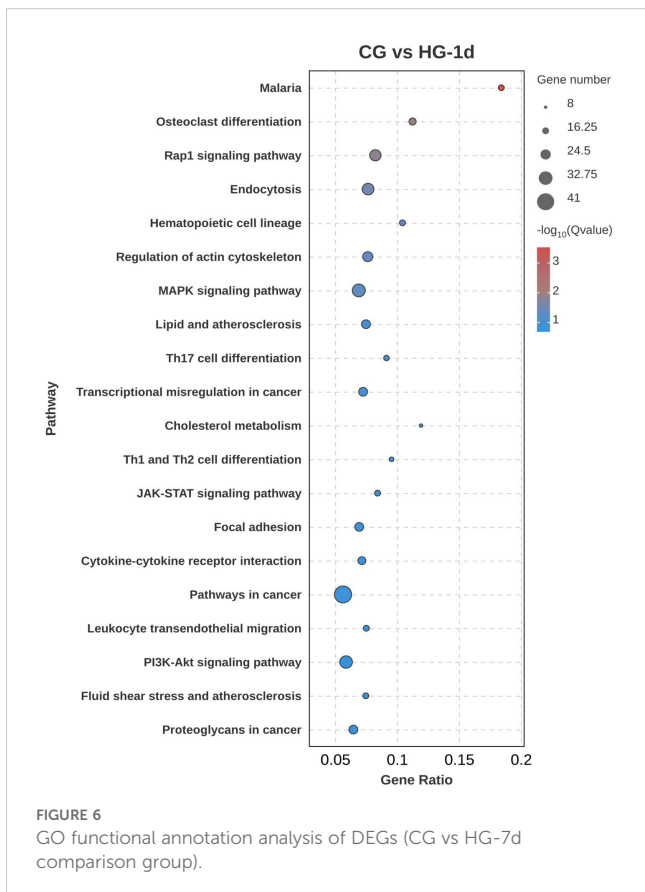GO functional annotation analysis of DEGs (CG vs HG-1d comparison group).

FIGURE 5
GO functional annotation analysis of DEGs (CG vs HG-4d comparison group).

FIGURE 6
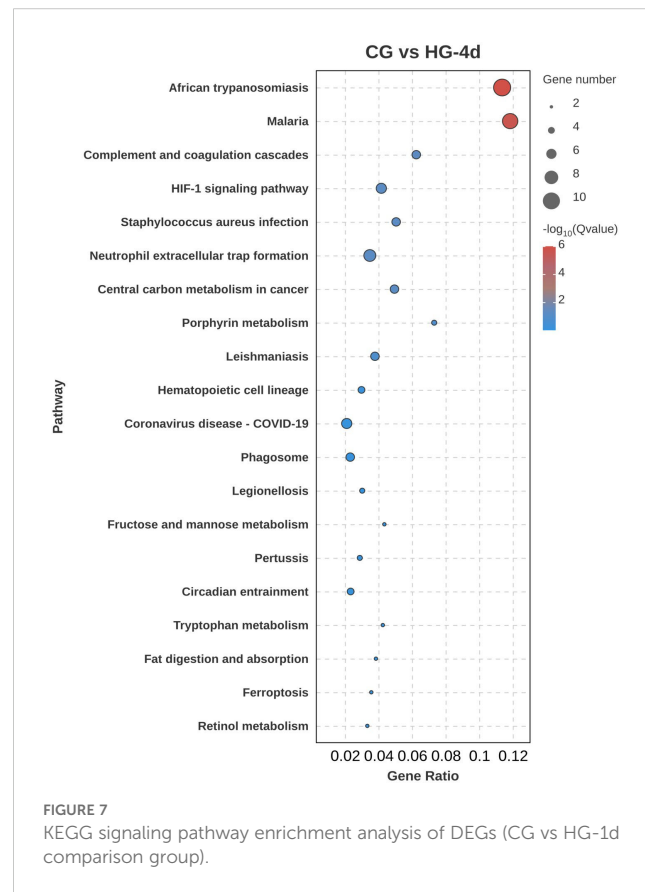GO functional annotation analysis of DEGs (CG vs HG-7d comparison group).

FIGURE 7
KEGG signaling pathway enrichment analysis of DEGs (CG vs HG-1d comparison group).

3.3.4 KEGG signaling pathway enrichment analysis results of DEGs

To further explore the biological functions of DEGs under hypoxic stress, KEGG pathway enrichment analysis was performed. In the CG vs HG-1d group (Figure 7), DEGs were mainly enriched in cancer pathways (ko05200), mitogen-activated protein kinase (MAPK) signaling pathway (ko04010), followed by endocytosis (ko04144), with 41, 31, and 28 DEGs annotated, respectively. In the CG vs HG-4d group (Figure 8), DEGs were mainly enriched in the HIF-1 signaling pathway (ko04066), phagosome signaling pathway (ko04145), and hematopoietic cell lineage (ko04640), with 6, 5, and 4 DEGs annotated, respectively. In the CG vs HG-7d group (Figure 9), DEGs were mainly enriched in regulation of actin cytoskeleton (ko04810), endocytosis signaling pathway (ko04144) with a large number of enriched DEGs, followed by Rap1 signaling pathway (ko04014), with 48, 46, and 45 DEGs annotated, respectively. Other enriched signaling pathways included the Ras signaling pathway (ko04014) and the JAK-STAT signaling pathway (ko04630).

3.3.5 Analysis of DEG expression trends

According to the expression patterns of 11,578 DEGs at different time points, they were clustered into 20 profiles. Among

these, five profiles, namely profile 17, profile 19, profile 15, profile 12, and profile 10, were significantly clustered ($p < 0.05$), containing 2,607, 1,675, 1,098, 780 and 877 DEGs, respectively (Figure 10). In profile 17, the expression pattern of DEGs first increased and then plateaued. In profile 19, the expression pattern of DEGs showed a continuous increasing trend. In profile 15, the expression pattern of DEGs first increased, then decreased, and then increased again. In profile 12, the expression pattern of DEGs first plateaued, then increased, and then plateaued again. In profile 10, the expression pattern of DEGs first plateaued and then increased. In addition, GO and KEGG enrichment analysis was performed on the genes in profile 17 and profile 19, and the results were similar to those obtained by the above DEG analysis.

3.4 Real-time fluorescence quantitative PCR verification results

To verify the accuracy of RNA-seq, 10 DEGs (five upregulated and five downregulated) were randomly selected for RT-qPCR quantitative verification. The results showed that although there were differences in the expression levels of up-regulated DEGs and down-regulated DEGs according to RT-qPCR quantification and
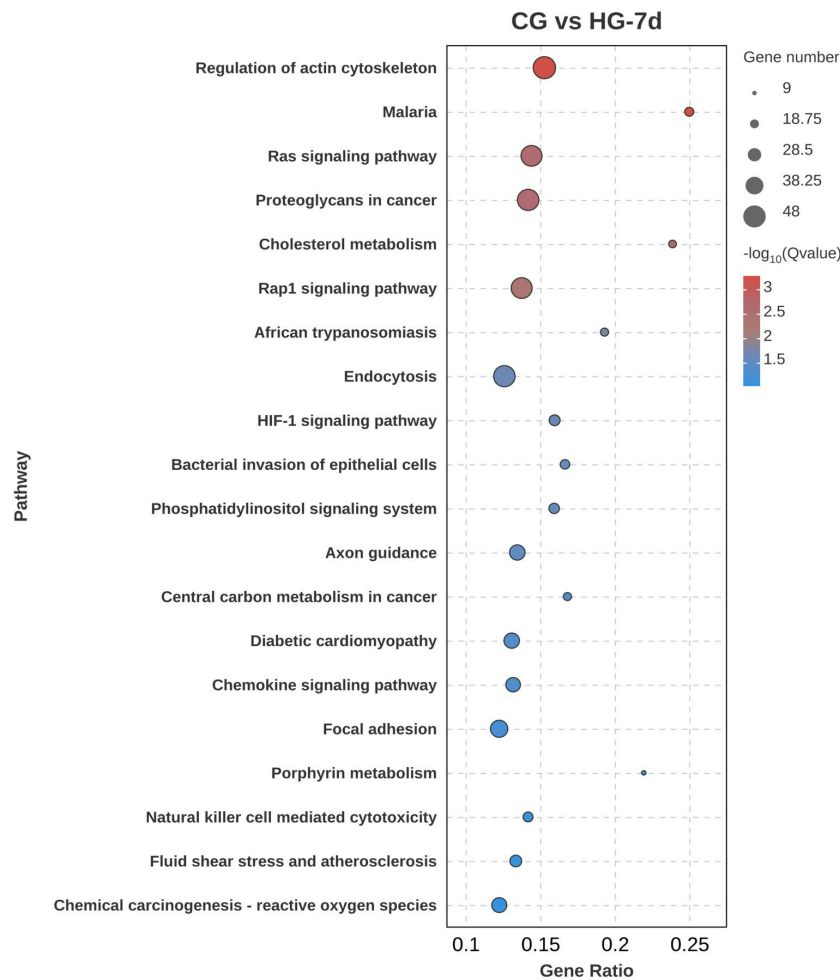

FIGURE 8
KEGG signaling pathway enrichment analysis of DEGs (CG vs HG-4d comparison group).
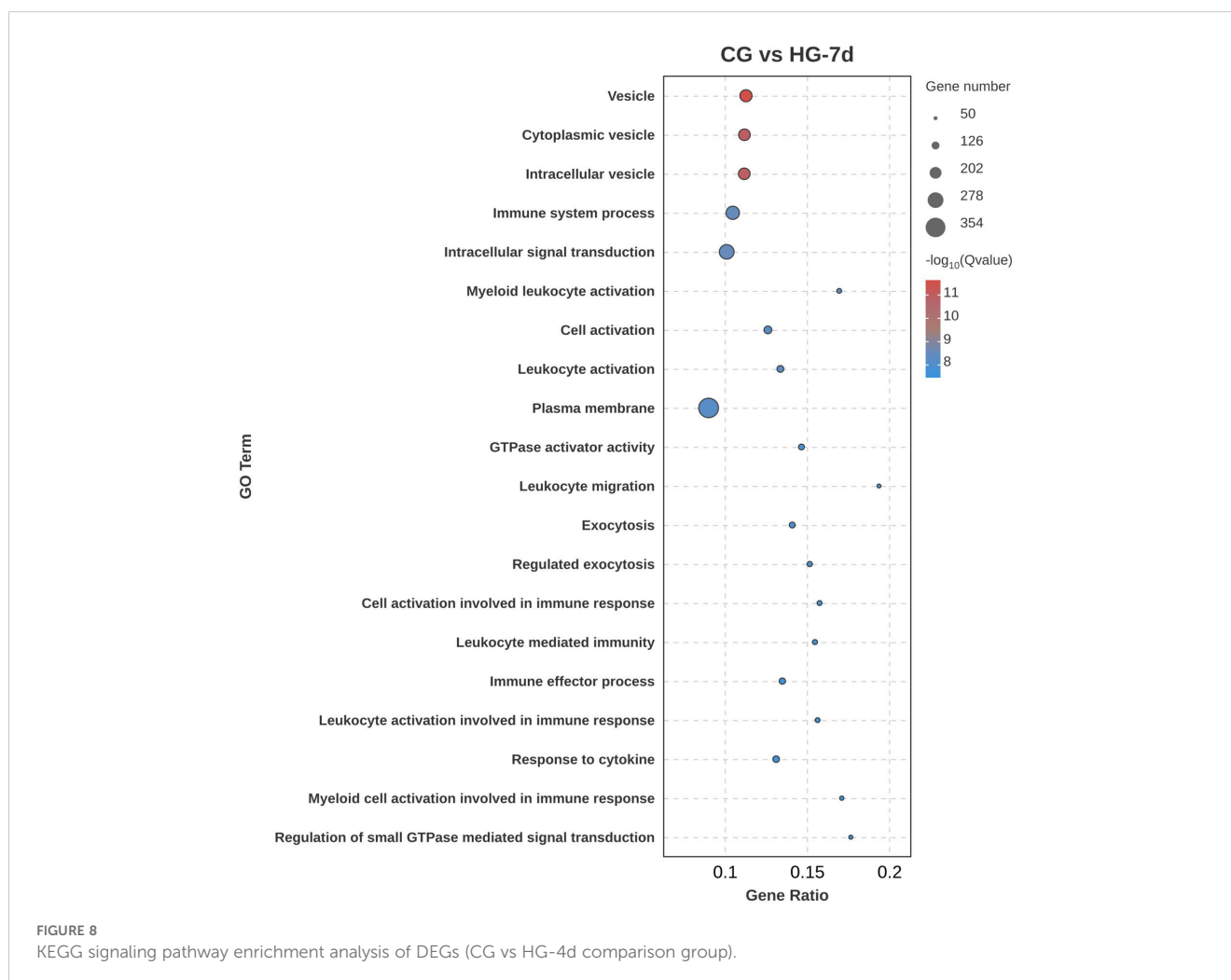
FIGURE 9
KEGG signaling pathway enrichment analysis of DEGs (CG vs HG-7d comparison group). Notes: Gene Ratio refers to the number of differentially expressed genes in the differentially expressed genes to the pathway divided by (/) the number of differentially expressed genes in the background genes enriched to the pathway.

RNA-seq expression, their change trends were consistent. This consistency proves that the results of RNA-seq were accurate and reliable and can be used for subsequent research and analysis (Figure 11).

4 Discussion

4.1 Effects of hypoxia stress on myocardial enzyme activities in the juvenile four-finger threadfin

The present study reveals significant variations in enzyme activities, including creatine kinase (CK), lactate dehydrogenase (LDH), and α-hydroxybutyrate dehydrogenase (HBDH), in the juvenile four-finger threadfin (*Eleutheronema tetradactylum*) under hypoxia. These findings align with previous research on hypoxia responses in various aquatic species, providing a contextual framework for understanding species-specific and conserved physiological mechanisms (Baldissera and Baldisserotto, 2023). In

Trachinotus ovatus, CK activity similarly showed significant increases under hypoxic conditions, indicating myocardial stress as a rapid adaptive mechanism to oxygen deficiency (Ou et al., 2014). Similarly, *Hypophthalmichthys molitrix* (silver carp) exhibited elevated serum LDH levels, highlighting damage to cardiac and other tissues under prolonged hypoxia (Ding et al., 2018). These responses suggest that CK and LDH serve as general markers of hypoxia-induced stress across teleosts, corroborating their diagnostic value in aquaculture management.

However, variations in enzyme responses among species also underscore distinct adaptive strategies. In bighead carp (*Hypophthalmichthys nobilis*), the increase in HBDH under hypoxia was less pronounced than in *E. tetradactylum*, potentially reflecting differences in metabolic reliance on aerobic pathways (Chen et al., 2021). This divergence may be attributed to ecological adaptations, as species inhabiting hypoxia-prone environments likely evolve mechanisms favoring anaerobic glycolysis. The time-dependent changes observed in *E. tetradactylum*, peaking enzyme activities around four days followed by partial normalization align with patterns in *Megalobrama amblycephala* (blunt snout bream),
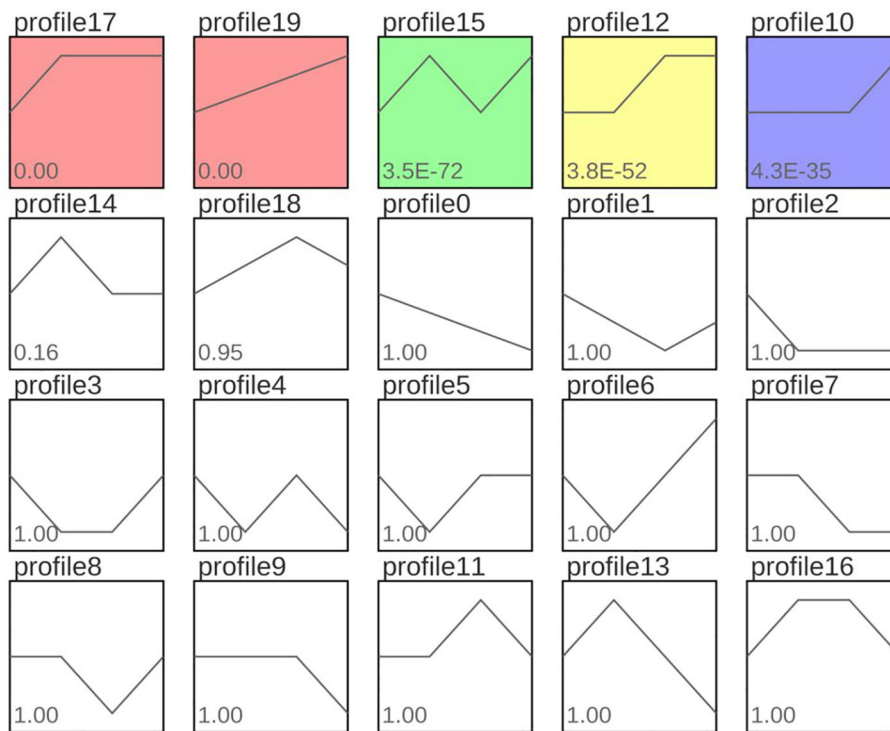
FIGURE 10

Expression trend analysis results of common DEGs in different comparison groups. Note: Profile17, profile19, profile15, profile12 and profile10 with red, green, yellow and purple backgrounds in the figure represent significant trends. Curves reflect changes in gene expression over time. The colored trend blocks indicate a trend of significant enrichment ($P<0.05$). Profile 17 and Profile 19 showed a trend of continuous upregulation; Profile 15 showed a trend of first upregulation, then downregulation, and finally upregulation; Profile 12 showed a trend of first leveling off and then upregulation. Profile 10 indicates a flattening trend followed by an upward adjustment.

where an initial surge in stress markers transitions into a stabilized metabolic state (Chen et al., 2017). This biphasic response highlights a shared ability among fish species to activate acute compensatory mechanisms before engaging longer-term structural and molecular adaptations (Farhana and Lappin, 2024). The results indicate that the myocardial enzyme activities in the four-finger threadfin are sensitive to hypoxia stress.

These enzymes are involved in the energy metabolism, with CK playing a crucial role in maintaining ATP levels through the creatine phosphate shuttle; LDH and HDBH are key enzymes in
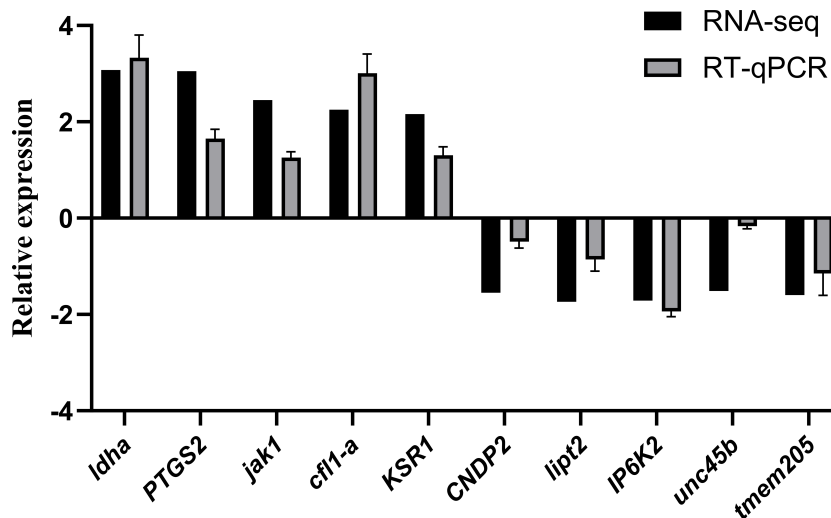

FIGURE 11

Validation of RNA-seq results by RT-qPCR.

anaerobic glycolysis and oxidative metabolism, respectively (Wallimann et al., 2011). The elevation of the levels of these enzymes may reflect the attempt of the fish heart to compensate for the reduced oxygen availability by enhancing anaerobic energy production and maximizing available ATP resources. The return of CK and LDH to baseline levels after 7 days of hypoxia suggest a shift towards metabolic exhaustion or a stabilization phase where the initial compensatory mechanisms are no longer effective; a further possibility is that the heart has adapted to hypoxic conditions. The sustained elevation in CK-MB and HDBH activities indicates that these enzymes might be more involved in long-term adaptations or stress responses to prolonged hypoxia (Kurapati and Soos, 2023). The myocardium of the four-finger threadfin shows a distinct, time-dependent response to hypoxia, with an initial increase in key enzyme activities, likely representing a compensatory mechanism initiated to sustain ATP production under reduced oxygen conditions. The peaking of enzyme activities at 4 days indicates a critical phase in the response to hypoxia, where metabolic demands are high and compensatory mechanisms are fully engaged. Research has shown that fish can adapt to hypoxic stress, and to maintain survival, the fish antioxidant system regulates its own physiology according to the environment (Jiang et al., 2015).

HDBH mainly exists in heart tissue. A significant increase in its activity means that the heart was damaged (Ye et al., 2024). In this study, after 4 days of hypoxic stress, the HDBH activity of the four-fingered threadfin was significantly higher than that of CG, indicating that hypoxia caused a certain degree of damage to the heart tissue. Its activity in tissues is much higher than in the blood. Elevated activity of LDH in the blood indicates that the structure of tissue cells such as the heart, liver, and muscles had been damaged (Anigol et al., 2023). In this study, the serum LDH levels in four-fingered threadfin were significantly higher than those in CG after being subjected to hypoxic stress, indicating that hypoxic stress caused a certain degree of damage to the heart, liver, and muscle tissues (Ma et al., 2023). Particularly CK-MB and HDBH activities can serve as biomarkers for chronic stress or as early indicators of potential myocardial damage in these fish (Popa et al., 2023; Omran et al., 2021). The increased levels of myocardial enzymes suggest they could serve as biomarkers to detect hypoxia-induced stress in aquaculture settings. By routinely monitoring these enzymes, farmers can assess the early stages of hypoxia exposure, allowing for timely intervention to mitigate adverse effects on fish health.These results underscore the importance of time for understanding the effects of hypoxia on fish physiology. Potential applications can improve aquaculture management and ensure the well-being of cultured species in environments prone to fluctuating oxygen levels.

4.2 Effects of hypoxia stress on cardiac tissue structure in juvenile four-finger threadfin

The heart is the most important energy supply organ in fish, and is closely related to the transport of substances, the stability of the internal environment, and the defense function of fish (Shaftoe

et al., 2023). Research has shown that hypoxia stress causes an increase in the gaps between myocardial cells in the heart of silver carp (*Hypophthalmichthys molitrix*), and disorder, swelling, and rupture of myocardial fibers (Li et al., 2021).

In this study, the rupture of myocardial fibers in juvenile four-finger threadfin became increasingly severe with the passage of time under hypoxia stress. The damage caused by hypoxia stress in four-fingered threadfin mainly manifested in the increase of the intercellular space between myocardial cells, disorder, swelling, and even rupture of myocardial fibers, which is consistent with relevant research results of the silver carp (Li et al., 2021). This study found substantial structural changes in the cardiac tissue of juvenile four-finger threadfin exposed to hypoxic conditions. In CG (Figure 2A), the myocardial fibers displayed a well-organized and continuous arrangement, with myocardial cells oriented in longitudinal, oblique, and circular bundles. This orderly structure is indicative of healthy cardiac tissue, in which cells are aligned to facilitate optimal contraction and function. In contrast, hypoxia-exposed groups (Figures 2B–D) exhibited progressive deterioration of the cardiac tissue structure. With increasing duration of hypoxic stress, intercellular gaps within the myocardium enlarged, and the muscle fibers became disordered. Swelling of myocardial fibers was observed, and in more severe cases, rupture of fibers occurred. This level of structural damage suggests that hypoxia imposes substantial stress on the cardiac tissue, disrupting the normal architecture and potentially impairing the functional capacity of the heart (Iwoń et al., 2024; Shati et al., 2022; Rocca et al., 2022; Burtscher et al., 2022; Su et al., 2021). The disorganization and swelling of myocardial fibers indicate cellular edema, which is a common response to hypoxic conditions. The rupture of muscle fibers in severe cases suggests that prolonged exposure to hypoxia may lead to irreversible damage, compromising the ability of the heart to contract effectively (Alvarenga et al., 2022; Cummins et al., 2019; Chaillou, 2018; Miller and Zachary, 2017). Prolonged hypoxia led to visible cardiac tissue damage, including disordered and ruptured myocardial fibers. Observing fish for symptoms like abnormal swimming behavior could indicate underlying hypoxia stress. Aquaculture practitioners could use behavioral observation alongside enzyme monitoring to gauge hypoxia levels in real-time.These findings align with the understanding that hypoxia disrupts cellular homeostasis, leads to tissue damage and potentially to long-term functional impairments.

4.3 Effects of hypoxia stress on the transcriptome of cardiac tissue in juvenile four-fingered threadfin

In aquaculture, hypoxia affects several physiological and biochemical enzymes, alters gene expression in key signal pathways, and impacts fish behavior, growth, immunity, and survival. Studying how four-fingered threadfin cope with hypoxia is essential for cultivating hypoxia-resistant varieties. The heart is a major organ susceptible to hypoxic stress. Research showed that hypoxic stress can cause myocardial hypertrophy in mammals, thereby changing both the composition of the extracellular matrix

and the myocardial metabolism (Gattuso et al., 2018). This study utilized high-throughput sequencing to compare the transcriptome and differentially expressed genes (DEGs) in cardiac tissues of four-fingered threadfin under hypoxia stress (1 d, 4 d, and 7 d) with a control group. The results revealed a predominance of upregulated genes across all groups, consistent with other species like *Megalobrama amblycephala* (Chen et al., 2017) and *Larimichthys crocea* (Mu et al., 2020). This indicates that the heart tissue responds to hypoxia primarily through increased gene expression, unlike gill tissue, which tends to inhibit gene expression under hypoxia (Zhang et al., 2023a, b).

This reduction in the number of DEGs from the 1-day to the 4-day group suggests that the organism is entering a phase of adaptation, where the acute stress response is being modulated. The smaller number of DEGs reflect a stabilization of gene expression patterns as the organism adjusts to the hypoxic environment. The high number of up-regulated genes suggests that the fish might be experiencing ongoing stress or that additional pathways are being activated in response to the prolonged hypoxic conditions. The concurrent increase in down-regulated genes also points to the repression of certain processes that are non-essential or even detrimental under prolonged hypoxic conditions.

In the early phase of the fish's adaptation to hypoxia, DEGs were predominantly associated with cell communication, cell periphery, and plasma membran. This association suggests that the initial response to hypoxia involves changes in the structural and communicative properties of cells, likely triggered to maintain cellular integrity and signaling under a hypoxic environment. The enrichments of catalytic activity, immune system process, and oxidoreductase activity suggest that the heart tissue had established a more robust cellular signaling and immune response, potentially with the aim to cope with prolonged hypoxic conditions (Burtscher et al., 2024; Mallet et al., 2022). Enrichment in the biological regulation, various vesicle-related processes, and cell activation further highlights the involvement of complex regulatory mechanisms, including vesicular transport and immune cell activation, which are critical for cellular adaptation and survival under hypoxic stress. The initial adaptation of the heart tissue to hypoxia involves considerable changes in the cellular component, particularly in cell communication, cell periphery, and plasma membrane structures (Zhao et al., 2023; Rocca et al., 2022; Lee et al., 2020). These changes likely reflect an immediate cellular response aimed to maintain communication and structural integrity under reduced oxygen availability. As hypoxia persists, a shift towards molecular functional adaptations can be observed, including upregulation of catalytic activities, immune responses, and oxidoreductase activities (Burtscher et al., 2024; Mallet et al., 2022). These changes suggest increasing metabolic demand and initiation of immune responses to counter the stress induced by prolonged hypoxic conditions. Prolonged exposure to hypoxia leads to further reinforcement of cellular signaling pathways, particularly those associated with plasma membrane and intracellular signal transduction (Bae et al., 2024; Ducsay et al., 2018).

The Mitogen-Activated Protein Kinase (MAPK) pathway plays a pivotal role in cellular responses to stress, including hypoxia.

Activation of MAPKs, such as ERK, JNK, and p38, triggers cascades that regulate cell survival, proliferation, and apoptosis. In this study, the MAPK pathway's enrichment indicates its role in the adaptive response to hypoxia by regulating stress-responsive genes (Chen et al., 2017). For instance, JNK activation under hypoxic stress mediates apoptosis and mitochondrial biogenesis, a crucial compensatory mechanism in myocardial cells (Bae et al., 2024). The involvement of cancer-related pathways suggests an early cellular response involving proliferation, survival, and apoptosis mechanisms, similar to those seen in tumorigenesis (Terekhanova et al., 2023; Ren et al., 2022; Bajrai et al., 2021). The activation of the MAPK pathway likely reflects a rapid stress response to maintain cellular homeostasis, while enrichment in endocytosis highlights the role of membrane dynamics and nutrient acquisition under low oxygen conditions (Guo et al., 2020).

The HIF-1 pathway is a key regulator of oxygen homeostasis. In hypoxic conditions, stabilization of HIF-1α promotes the transcription of genes like VEGFA and LDHA, enhancing angiogenesis and anaerobic glycolysis (Wu et al., 2023). Upregulation of VEGFA in your study suggests enhanced vascular remodeling, critical for improving oxygen delivery to cardiac tissues under hypoxic stress. HIF-1 plays a critical role in cellular adaptation to hypoxia by regulating oxygen homeostasis, metabolism, and angiogenesis (Yfantis et al., 2023; Infantino et al., 2020). The activation of the phagosome pathway suggests enhanced cellular mechanisms for removing damaged cells or pathogens. The involvement of hematopoietic pathways indicates a potential compensatory response to enhance oxygen transport by increasing blood cell production (Westman et al., 2020; Lee P. et al., 2020). This response may be essential for maintaining cellular integrity during prolonged stress. Enrichment in hematopoietic pathways suggests that prolonged hypoxia may impact blood cell formation, which could be a compensatory response to enhance the oxygen transport capacity of the fish (Rhodes et al., 2022).

The regulation of the actin cytoskeleton pathway, enriched on Day 7, highlights its role in maintaining cellular integrity under prolonged hypoxia. Actin remodeling facilitates cellular motility and structural integrity, essential for tissue repair and survival during hypoxic stress (Tang and Gerlach, 2017). GO enrichment of immune system processes reflects the activation of cellular defense mechanisms. Increased phagosome activity suggests enhanced autophagic responses to clear damaged organelles and maintain cellular homeostasis (Westman et al., 2020). The regulation of the actin cytoskeleton reflects necessary structural adjustments in cells to cope with sustained stress (Tang and Gerlach, 2017). The continued enrichment of endocytosis further emphasizes its role in cellular remodeling and nutrient acquisition. Rap1 signaling, involved in cell adhesion, growth, and differentiation, indicates a need for more extensive signaling modifications under prolonged hypoxic conditions (Gibieža and Petrikaitė, 2021; López-Hernández et al., 2020; Hilbi and Kortholt, 2017). Rap1 signaling modulates cell adhesion and vascular permeability, crucial under hypoxia for maintaining tissue integrity (Xie et al., 2024; Yu et al., 2021; López-Hernández et al., 2020). Concurrently, the PI3K/Akt pathway, enriched in this study, supports cell survival and energy homeostasis by upregulating anti-

apoptotic proteins and promoting glycolysis (Hu et al., 2023; Sarapultsev et al., 2023; Rah et al., 2022; Gehringer et al., 2020). These genes play crucial roles in cell metabolism, growth regulation, immune response, and glucose metabolism (Gehringer et al., 2020; Weir and Olschewski, 2006). The dynamic and time-dependent gene regulation in response to hypoxia in juvenile four-finger threadfin is characterized by early activation of stress and survival pathways, a mid-stage shift towards immune and oxygen homeostasis mechanisms, and long-term structural and metabolic adjustments. These responses highlight the complex interplay of signaling pathways aimed at maintaining cellular integrity and function under sustained hypoxic stress.

Hypoxia-inducible factor-1 (HIF-1) is a key pathway in fish response to hypoxic stress, playing a vital role in adaptive strategies by regulating basal metabolism, inhibiting red blood cell proliferation, and stimulating compensatory mechanisms like angiogenesis (Elbassiouny et al., 2024). In this study, 23 genes were significantly enriched in the HIF-1 signaling pathway, with important genes such as *HO-1*, *LDH*, *HK*, and *VEGFA* upregulated ($P < 0.05$). The gene *HO-1*, a downstream target of HIF-1, plays a critical role in protecting against oxidative stress by generating carbon monoxide, biliverdin, and free iron during the breakdown of heme. These products have antioxidant and anti-inflammatory effects in both *in vitro* and *in vivo* models of stress and organ injury (Xie et al., 2021; Lin et al., 2019; Kim et al., 2006). Lactate dehydrogenase-A (*LDH-A*), a key enzyme in glycolysis (Sharma et al., 2022), was significantly upregulated in the heart of juvenile four-fingered threadfin, indicating enhanced anaerobic metabolism under hypoxic conditions (Wu et al., 2023; Pei et al., 2021). Moreover, vascular endothelial growth factor A (*VEGFA*) is upregulated during hypoxia, promoting angiogenesis and enhancing oxygen delivery by increasing blood vessel formation and regulating cell proliferation. *VEGFA*'s role in the response to hypoxic stress suggests that four-fingered threadfin enhance their oxygen delivery capacity through increased angiogenesis. The enrichment of genes related to metabolic pathways, such as the HIF-1 signaling pathway and anaerobic glycolysis, suggests metabolic shifts under hypoxic conditions. Feed formulations tailored to these metabolic needs, emphasizing easily digestible proteins and energy sources, can help optimize fish health and growth. Nutritional adjustments could support energy production in hypoxia-prone environments, improving overall efficiency.

Transcriptomic analysis revealed a marked upregulation of genes associated with the HIF-1 and MAPK signaling pathways in *E. tetradactylum*, indicative of metabolic shifts to enhance anaerobic energy production and maintain cellular integrity under hypoxic conditions. These pathways have also been identified in cobia (*Rachycentron canadum*), Eurasian perch (*Perca fluviatilis*) (Rimoldi et al., 2012). and large yellow croaker (*Larimichthys crocea*) as central to hypoxia tolerance. The activation of the HIF-1 pathway supports adaptive processes like angiogenesis and glycolysis, as evidenced by upregulated VEGFA and LDHA genes in both species (Xie et al., 2021; Rimoldi et al., 2012). In *Larimichthys crocea* (large yellow croaker), hypoxia-responsive pathways such as

hypoxia-inducible factor-1 (HIF-1) signaling and MAPK pathways were significantly upregulated, similar to the findings in *E. tetradactylum* (Mu et al., 2020). These pathways are pivotal for cellular survival under hypoxia, underscoring conserved genetic and signaling mechanisms that transcend species boundaries. The identification of hypoxia-responsive genes, particularly those involved in energy metabolism and oxidative stress, highlights candidate genes that could be targeted in selective breeding programs to develop hypoxia-resilient strains of *E. tetradactylum*. By selectively breeding individuals with favorable expressions of these genes, aquaculture can enhance the resilience of fish populations in environments prone to low oxygen conditions.

The comparison between RNA-seq and RT-qPCR results demonstrates consistency in gene expression trends, despite differences in absolute expression levels. RNA-seq, a high-throughput, genome-wide method, and RT-qPCR, a targeted, highly sensitive technique, both identified similar patterns of upregulated and downregulated genes. Differences in methodologies, including sample preparation and sensitivity, contribute to discrepancies in expression levels, but the consistent directional changes (upregulation or downregulation) between the two methods validate the RNA-seq results (Micheel et al., 2024; Aguiar et al., 2023). RT-qPCR validation of 10 DEGs confirmed these trends, underscoring the reliability of the RNA-seq data for further analysis. This consistency supports RNA-seq as a dependable tool for studying gene expression changes under experimental conditions (Sampathkumar et al., 2022).

5 Conclusion

This study investigates the effects of hypoxic stress on myocardial enzyme activity, cardiac tissue structure, and gene expression in juvenile four-finger threadfin (*Eleutheronema tetradactylum*) over various exposure periods. Hypoxic stress led to a significant increase in CK, CK-MB, HDBH, and LDH levels, indicating cardiac stress. Histological analysis revealed increased gaps between myocardial cells, and myocardial fibers became disordered, swollen, and ruptured with prolonged hypoxia exposure. Transcriptome analysis identified differentially expressed genes (DEGs) primarily enriched in the phosphatidylinositol signaling pathway, endocytosis, Rap1 signaling pathway, regulation of the actin cytoskeleton, and MAPK signaling pathway. Hypoxia induced the upregulation of genes such as *HO-1*, *LDHA*, and *VEGFA*, indicating the heart's self-protection mechanisms. Notably, the PI3K-Akt and MAPK signaling pathways were enriched, suggesting their role in reducing hypoxic damage. The study revealed dynamic changes in gene expression over time. An initial upregulation of stress-related genes was observed, followed by stabilization around day 4, and reactivation of stress-adaptive pathways by day 7, suggesting a shift toward chronic stress responses. Immune system processes remained significantly enriched, underscoring the importance of sustained immune responses in hypoxia adaptation. The temporal pattern of pathway enrichment transitioned from early protective responses (e.g.,

MAPK signaling and cancer pathways) to specialized adaptations (e.g., HIF-1 signaling and actin cytoskeleton regulation). The clustering of DEGs into distinct temporal profiles highlighted complex gene expression dynamics, with different groups of genes activated at various stages of hypoxia response. This study emphasizes the vulnerability of cardiac tissue to hypoxic stress and the progressive structural damage in the heart with prolonged exposure. The findings suggest that while four-finger threadfin can adapt to some extent by day 4, chronic hypoxia triggers additional gene expression changes, potentially signaling a shift to alternative survival pathways. This study enhances understanding of hypoxia effects on juvenile four-finger threadfin, offering insights to improve fish welfare, productivity, and resilience in aquaculture. Key findings, like hypoxia-responsive genes, support selective breeding and real-time monitoring, advancing sustainable practices, reducing stress, and promoting adaptive systems for food security and environmental conservation.The study underscores the significance of regulatory pathways, such as the immune system and cell membrane processes, in the heart's response to hypoxia. This dynamic and time-dependent adaptation offers key insights into how aquatic species might survive under prolonged hypoxic conditions and suggests potential research targets for conservation efforts in hypoxia-sensitive species.

This study highlights key insights from transcriptomic analysis but is limited by the absence of proteomics and metabolomics, which could uncover additional molecular and post-transcriptional mechanisms. The laboratory conditions may not fully replicate natural aquaculture environments, and the findings are species-specific. Future research should integrate proteomics, metabolomics, and epigenomics for a broader understanding of hypoxia responses, conduct studies in real aquaculture settings, and explore hypoxia adaptation in other commercially important species. These efforts will enhance the understanding of hypoxia adaptation and support the development of resilient aquaculture systems.

Data availability statement

The raw data supporting the conclusions of this article will be made available by the authors, without undue reservation.

Ethics statement

The use of all animals in this project was conducted under the Animal Welfare Act, the PHS Animal Welfare Policy, the National Institutes of Health (NIH) Guide for Care and Use of Laboratory Animals, and the policies and procedures of the People's Republic of China, Guangdong province, and Guangdong Ocean University. The study was conducted in compliance with the regulations for administering laboratory animals in Guangdong province, China, and in compliance with the Guangdong Ocean University Research Council's guidelines for the care and use of laboratory animals (approval number: GDOU-LAE-2023-015). The study was conducted in accordance with the local legislation and institutional requirements.

Author contributions

YL: Data curation, Formal analysis, Investigation, Methodology, Project administration, Software, Validation, Visualization, Writing – original draft, Writing – review & editing. EA: Data curation, Formal analysis, Methodology, Software, Validation, Visualization, Writing – original draft, Writing – review & editing. YY: Data curation, Methodology, Software, Validation, Visualization, Writing – original draft. ZW: Data curation, Resources, Supervision, Validation, Writing – review & editing. JJ: Data curation, Software, Validation, Visualization, Writing – review & editing. RX: Data curation, Software, Supervision, Validation, Visualization, Writing – original draft. ED: Data curation, Software, Validation, Visualization, Writing – review & editing. JH: Conceptualization, Data curation, Formal analysis, Funding acquisition, Methodology, Resources, Software, Supervision, Validation, Visualization, Writing – original draft, Writing – review & editing.

Conflict of interest

Author RX was employed by the company Guangdong Evergreen Feed Industry Co. Ltd.

The remaining authors declare that the research was conducted in the absence of any commercial or financial relationships that could be constructed as a potential conflict of interest.

The author(s) declared that they were an editorial board member of Frontiers, at the time of submission. This had no impact on the peer review process and the final decision.

Generative AI statement

The author(s) declare that no Generative AI was used in the creation of this manuscript.

Publisher's note

All claims expressed in this article are solely those of the authors and do not necessarily represent those of their affiliated organizations, or those of the publisher, the editors and the reviewers. Any product that may be evaluated in this article, or claim that may be made by its manufacturer, is not guaranteed or endorsed by the publisher.

References

Aguiar, V. R. C., Castelli, E. C., Single, R. M., Bashirova, A., Ramsuran, V., Kulkarni, S., et al. (2023). Comparison between qPCR and RNA-seq reveals challenges of quantifying HLA expression. *Immunogenetics* 75, 249–262. doi: 10.1007/s00251-023-01296-7

Ali, B., Anushka,, and Mishra, A. (2022). Effects of dissolved oxygen concentration on freshwater fish: A review. *Int. J. Fish. Aquat. Stud.* 10, 113–127. doi: 10.22271/fish.2022.v10.i4b.2693

Alvarenga, M. G., Nobrega, J., Cerqueira, R. J., and Mancio, J. (2022). Myocardial oedema: Pathophysiological basis and implications for the failing heart. *ESC Heart Failure* 9, 958–976. doi: 10.1002/ehf2.13775

Anigol, S. S., Neglur, S. B., and Muniswamy, D. (2023). Blood glucose and glycogen levels as indicators of stress in the freshwater fish, *Cirrihinus mrigal* under Cyphenothrin intoxication. *Toxicol. Int.* 30, (51). doi: 10.18311/ti/2023/v30i1/30444

Bae, T., Hallis, S. P., and Kwak, M. (2024). Hypoxia, oxidative stress, and the interplay of HIFs and NRF2 signaling in cancer. *Exp. Mol. Med.* 56, 501–514. doi: 10.1038/s12276-024-01180-8

Bajrai, L. H., Sohrab, S. S., Mobashir, M., Kamal, M. A., Rizvi, M. A., and Azhar, E. I. (2021). Understanding the role of potential pathways and its components including hypoxia and immune system in case of oral cancer. *Sci. Rep.* 11, 1–10. doi: 10.1038/s41598-021-98031-7

Baldissera, M. D., and Baldisserotto, B. (2023). Creatine kinase activity as an indicator of energetic impairment and tissue damage in fish: A review. *Fishes* 8, 59. doi: 10.3390/fishes8020059

Burtscher, J., Niedermeier, M., Hüfner, K., Van den Burg, E., Kopp, M., Stoop, R., et al. (2022). The interplay of hypoxic and mental stress: Implications for anxiety and depressive disorders. *Neurosci. Biobehav. Rev.* 138, 104718. doi: 10.1016/j.neubiorev.2022.104718

Burtscher, J., Pasha, Q., Chanana, N., Millet, G. P., Burtscher, M., and Strasser, B. (2024). Immune consequences of exercise in hypoxia: A narrative review. *J. Sport Health Sci.* 13 (3), 297–310. doi: 10.1016/j.jshs.2023.09.007

Canosa, L. F., and Bertucci, J. I. (2023). The effect of environmental stressors on growth in fish and its endocrine control. *Front. Endocrinol.* 14. doi: 10.3389/fendo.2023.1109461

Cerra, M. C., Filice, M., Caferro, A., Mazza, R., Gattuso, A., and Imbrogno, S. (2023). Cardiac hypoxia tolerance in fish: from functional responses to cell signals. *Int. J. Mol. Sci.* 24, 1460. doi: 10.3390/ijms24021460

Chaillou, T. (2018). Skeletal muscle fiber type in hypoxia: adaptation to high-altitude exposure and under conditions of pathological hypoxia. *Front. Physiol.* 9. doi: 10.3389/fphys.2018.01450

Chen, G., Pang, M., Yu, X., Wang, J., and Tong, J. (2021). Transcriptome sequencing provides insights into the mechanism of hypoxia adaption in bighead carp (*Hypophthalmichthys nobilis*). *Comp. Biochem. Physiol. Part D: Genomics Proteomics* 40, 100891. doi: 10.1016/j.cbd.2021.100891

Chen, B., Yi, S., Wang, W., He, Y., Huang, Y., Gao, Z., et al. (2017). Transcriptome comparison reveals insights into muscle response to hypoxia in blunt snout bream (*Megalobrama amblycephala*). *Gene* 624, 6–13. doi: 10.1016/j.gene.2017.04.023

Cummins, E. P., Strowitzki, M. J., and Taylor, C. T. (2019). Mechanisms and consequences of oxygen and carbon dioxide sensing in mammals. *Physiol. Rev.* 100, 463–488. doi: PRV-00003-2019

Ding, C. Y., Hu, L. S., Li, Y., Xue, Y., Li, H., Wu, R. H., et al. (2018). Effects of hypoxia stress on cardiomyocyte apoptosis and the control for Bax, Bcl-2 expressions in *Hypophthalmichthys molitrix*. *Freshw. Fisheries* 48, 10–15.

Doenst, T., Nguyen, T. D., and Abel, E. D. (2013). Cardiac metabolism in heart failure: implications beyond ATP production. *Circ. Res.* 113, 709–724. doi: 10.1161/CIRCRESAHA.113.300376

Ducsay, C. A., Goyal, R., Pearce, W. J., Wilson, S., Hu, Q., and Zhang, L. (2018). Gestational hypoxia and developmental plasticity. *Physiol. Rev.* 98, 1241–1334. doi: 10.1152/physrev.00043.2017

Elbassiouny, A. A., Buck, L. T., Abatti, L. E., Mitchell, J. A., Crampton, W. G. R., Lovejoy, N. R., et al. (2024). Evolution of a novel regulatory mechanism of hypoxia inducible factor in hypoxia-tolerant electric fishes. *J. Biol. Chem.* 300, 105727. doi: 10.1016/j.jbc.2024.105727

Essop, M. F. (2007). Cardiac metabolic adaptations in response to chronic hypoxia. *J. Physiol.* 584, 715–726. doi: 10.1113/jphysiol.2007.143511

Everett, M. V., Antal, C. E., and Crawford, D. L. (2012). The effect of short-term hypoxic exposure on metabolic gene expression. *J. Exp. Zool. Part A: Ecol. Genet. Physiol.* 317A, 9–23. doi: 10.1002/jez.717

Farhana, A., and Lappin, S. L. (2024). "Biochemistry, lactate dehydrogenase," in *StatPearls* (StatPearls Publishing, Treasure Island (FL). Available at: https://www.ncbi.nlm.nih.gov/books/NBK557536/.

Galli, G. L. J., Lock, M. C., Smith, K. L. M., and Giussani, D. A. (2023). Effects of developmental hypoxia on the vertebrate cardiovascular system. *Physiology.* 38 (2), 53–62. doi: 10.1152/physiol.00022.2022

Gattuso, A., Garofalo, F., Cerra, M. C., and Imbrogno, S. (2018). Hypoxia tolerance in teleosts: implications of cardiac nitrosative signals. *Front. Physiol.* 9. doi: 10.3389/fphys.2018.00366

Gehringer, F., Weissinger, S. E., Möller, P., Wirth, T., and Ushmorov, A. (2020). Physiological levels of the PTEN-PI3K-AKT axis activity are required for maintenance of Burkitt lymphoma. *Leukemia* 34, 857–871. doi: 10.1038/s41375-019-0628-0

Gibieža, P., and Petrikaitè, V. (2021). The regulation of actin dynamics during cell division and Malignancy. *Am. J. Cancer Res.* 11, 4050–4069. Available at: https://www.ncbi.nlm.nih.gov/pmc/articles/PMC8493394/.

Gu, Y., Sun, J. L., Yao, F. C., Jiang, T., Jin, C. X., Shi, L. P., et al. (2023). Long-term hypoxia and reoxygenation induced oxidative stress lead to immunosuppression and apoptosis in golden pompano (*Trachinotus blochii*). *Front. Mar. Sci.* 10. doi: 10.3389/fmars.2023.1212571

Guo, J., Pan, W., Liu, B., Shen, F., Xu, Y., and Hu, L. (2020). ERK/MAPK signalling pathway and tumorigenesis. *Exp. Ther. Med.* 19, 1997–2007. doi: 10.3892/etm.2020.8454

Hilbi, H., and Kortholt, A. (2017). Role of the small GTPase Rap1 in signal transduction, cell dynamics and bacterial infection. *Small GTPases* 10, 336–342. doi: 10.1080/21541248.2017.1331721

Hu, Q., Bian, Q., Rong, D., Wang, L., Song, J., Huang, S., et al. (2023). JAK/STAT pathway: Extracellular signals, diseases, immunity, and therapeutic regimens. *Front. Bioeng. Biotechnol.* 11. doi: 10.3389/fbioe.2023.1110765

Huang, J., Guo, Z., Zhang, J., Wang, W., Wang, Z., Amenyogbe, E., et al. (2021). Effects of hypoxia-reoxygenation conditions on serum chemistry indicators and gill and liver tissues of cobia (*Rachycentron canadum*). *Aquacult. Rep.* 20, 100692. doi: 10.1016/j.aqrep.2021.100692

Huang, J.-S., Guo, Z.-X., Zhang, J.-D., Wang, W.-Z., Wang, Z.-L., Xie, R.-T., et al. (2023). Transcriptomic analysis of juvenile cobia in response to hypoxic stress. *Aquacult. Int.* 31, 931–955. doi: 10.1007/s10499-022-01007-1

Infantino, V., Santarsiero, A., Convertini, P., Todisco, S., and Iacobazzi, V. (2020). Cancer cell metabolism in hypoxia: role of HIF-1 as key regulator and therapeutic target. *Int. J. Mol. Sci.* 22, 5703. doi: 10.3390/ijms22115703

Iqbal, T. H., Hajisamae, S., Lim, A., Jantarat, S., Wang, X., and Tsim, W. K. (2023). Feeding habits of four-finger threadfin, *Eleutheronema tetradactylum*, and its diet interaction with co-existing fish species in the coastal waters of Thailand. *PeerJ* 11, e14688. doi: 10.7717/peerj.14688

Iwoń, Z., Krogulec, E., Kierlańczyk, A., Wojasiński, M., and Jastrzębska, E. (2024). Hypoxia and re-oxygenation effects on human cardiomyocytes cultured on polycaprolactone and polyurethane nanofibrous mats. *J. Biol. Eng.* 18, 37. doi: 10.1186/s13036-024-00432-5

Jiang, X., Dong, S., Liu, R., Huang, M., Dong, K., Ge, J., et al. (2021). Effects of temperature, dissolved oxygen, and their interaction on the growth performance and condition of rainbow trout (*Oncorhynchus mykiss*). *J. Thermal Biol.* 98, 102928. doi: 10.1016/j.jtherbio.2021.102928

Jiang, H. P., Zhang, C., Wang, C. C., and Xu, Q. H. (2015). Cloning of HIF1B and HIF2A to hypoxia in Gymnocypris genes and their expressions response dobula and *Schizothorax prenanti*. *Freshw. Fisheries* 45, 11–18.

Kim, J., Tchernyshyov, I., Semenza, G. L., and Dang, C. V. (2006). HIF-1-mediated expression of pyruvate dehydrogenase kinase: A metabolic switch required for cellular adaptation to hypoxia. *Cell Metab.* 3, 177–185. doi: 10.1016/j.cmet.2006.02.002

Kurapati, R., and Soos, M. P. (2023). "CPK-MB," in *StatPearls* (StatPearls Publishing, Treasure Island (FL). Available at: https://www.ncbi.nlm.nih.gov/books/NBK557591/.

Lee, P., Chandel, N. S., and Simon, M. C. (2020). Cellular adaptation to hypoxia through HIFs and beyond. *Nat. Rev. Mol. Cell Biol.* 21, 268. doi: 10.1038/s41580-020-0227-y

Lee, J., Woo, Y., Hahn, W., Jung, Y. M., and Jung, J. (2020). Formation and maturation of the phagosome: A key mechanism in innate immunity against intracellular bacterial infection. *Microorganisms* 8 (9), 1298. doi: 10.3390/microorganisms8091298

Li, X., Li, F., Zou, G., Feng, C., Sha, H., Liu, S., et al. (2021). Physiological responses and molecular strategies in heart of silver carp (*Hypophthalmichthys molitrix*) under hypoxia and reoxygenation. *Comp. Biochem. Physiol. Part D: Genomics Proteomics* 40, 100908. doi: 10.1016/j.cbd.2021.100908

Li, G., Liu, B., Yang, J., Li, X., Wang, H., Wen, H., et al. (2022). Acute hypoxia stress-induced apoptosis in gill of Japanese flounder (*Paralichthys olivaceus*) by modulating the epas1/bad pathway. *Biology* 11 (11), 1656. doi: 10.3390/biology11111656

Lin, C., Hsiao, L., Cho, R., and Yang, C. (2019). CO-releasing molecule-2 induces nrf2/ARE-dependent heme oxygenase-1 expression suppressing TNF-α-induced pulmonary inflammation. *J. Clin. Med.* 8, 436. doi: 10.3390/jcm8040436

Liu, B., Li, G., Li, X., Wang, H., Yang, J., Wen, H., et al. (2024). The responsive mechanisms of DNA methylation and transcriptional regulation to acute hypoxia stress in HIF-1/VEGFA signal pathway of Japanese flounder (*Paralichthys olivaceus*). *Aquaculture* 578, 740021. doi: 10.1016/j.aquaculture.2023.740021

Liu, S., Wang, X., Sun, F., Zhang, J., Feng, J., Liu, H., et al. (2013). RNA-Seq reveals expression signatures of genes involved in oxygen transport, protein synthesis, folding, and degradation in response to heat stress in catfish. *Physiol. Genomics*. 45, 462–476 . doi: 10.1152/physiolgenomics.00026.2013

López-Hernández, T., Haucke, V., and Maritzen, T. (2020). Endocytosis in the adaptation to cellular stress. *Cell Stress* 4, 230–247. doi: 10.15698/cst2020.10.232

Ma, Q., Luo, Y., Zhong, J., Limbu, S. M., Li, Y., Chen, Q., et al. (2023). Hypoxia tolerance in fish depends on catabolic preference between lipids and carbohydrates. *Zoological Res.* 44, 954–966. doi: 10.24272/j.issn.2095-8137.2023.098

Mallet, R. T., Burtscher, J., Pialoux, V., Pasha, Q., Ahmad, Y., Millet, G. P., et al. (2022). Molecular mechanisms of high-altitude acclimatization. *Int. J. Mol. Sci.* 24, 1698. doi: 10.3390/ijms24021698

Micheel, J., Safrastyan, A., Aron, F., and Wollny, D. (2024). Exploring the impact of primer length on efficient gene detection via high-throughput sequencing. *Nat. Commun.* 15, 1–9. doi: 10.1038/s41467-024-49685-0

Miller, M. A., and Zachary, J. F. (2017). Mechanisms and morphology of cellular injury, adaptation, and death. *Pathologic Basis Veterinary Dis.* 2–43.e19. doi: 10.1016/B978-0-323-35775-3.00001-1

Mu, Y., Li, W., Wei, Z., He, L., Zhang, W., and Chen, X. (2020). Transcriptome analysis reveals molecular strategies in gills and heart of large yellow croaker (*Larimichthys crocea*) under hypoxia stress. *Fish. Shellfish Immunol.* 104, 304–313. doi: 10.1016/j.fsi.2020.06.028

Noureen, A., Jabeen, F., Wajid, A., Kazim, M. Z., Safdar, N., and Cappello, T. (2023). Natural bioactive phytocompounds to reduce toxicity in common carp *cyprinus carpio*: A challenge to environmental risk assessment of nanomaterials. *Water* 15, 1152. doi: 10.3390/w15061152

Omran, F., Kyrou, I., Osman, F., Lim, V. G., Randeva, H. S., and Chatha, K. (2021). Cardiovascular biomarkers: lessons of the past and prospects for the future. *Int. J. Mol. Sci.* 23, 5680. doi: 10.3390/ijms23105680

Ošťádal, B., and Kolář, F. (1999). "Myocardial Hypoxia and Ischemia," in *Cardiac Ischemia: From Injury to Protection. Basic Science for the Cardiologist*, vol. 4. (Springer, Boston, MA). doi: 10.1007/978-1-4757-3025-8_1

Ou, Y., Fan, C., Li, J., Yu, N., and Su, H. (2014). Acute hypoxia stress on blood biochemical indexes in selective group of *Trachinotus ovatus*. *Acta Oceanologica Sin.* 36, 126–131.

Pei, X., Chu, M., Tang, P., Zhang, H., Zhang, X., Zheng, X., et al. (2021). Effects of acute hypoxia and reoxygenation on oxygen sensors, respiratory metabolism, oxidative stress, and apoptosis in hybrid yellow catfish "Huangyou-1. *Fish. Physiol. Biochem.* 47, 1429–1448. doi: 10.1007/s10695-021-00989-8

Popa, D. M., Macovei, L., Moscalu, M., Sascău, R. A., and Stătescu, C. (2023). The prognostic value of creatine kinase-MB dynamics after primary angioplasty in ST-elevation myocardial infarctions. *Diagnostics* 13 (19), 3143. doi: 10.3390/diagnostics13193143

Rah, B., Rather, R. A., Bhat, G. R., Baba, A. B., Mushtaq, I., Farooq, M., et al. (2022). JAK/STAT signaling: molecular targets, therapeutic opportunities, and limitations of targeted inhibitions in solid Malignancies. *Front. Pharmacol.* 13. doi: 10.3389/fphar.2022.821344

Rao, X., Huang, X., Zhou, Z., and Lin, X. (2013). An improvement of the 2ˆ(–delta delta CT) method for quantitative real-time polymerase chain reaction data analysis. *Biostatistics Bioinf. Biomathematics* 3, 71. Available at: https://www.ncbi.nlm.nih.gov/pmc/articles/PMC4280562/.

Ren, X., Cui, H., Wu, J., Zhou, R., Wang, N., Liu, D., et al. (2022). Identification of a combined apoptosis and hypoxia gene signature for predicting prognosis and immune infiltration in breast cancer. *Cancer Med.* 11, 3886–3901. doi: 10.1002/cam4.4755

Rhodes, C. E., Denault, D., and Varacallo, M. (2022). "Physiology, oxygen transport," in *StatPearls* (StatPearls Publishing, Treasure Island (FL). Available at: https://www.ncbi.nlm.nih.gov/books/NBK538336/.

Rimoldi, S., Terova, G., Ceccuzzi, P., Marelli, S., Antonini, M., and Saroglia, M. (2012). HIF-1α mRNA levels in Eurasian perch (*Perca fluviatilis*) exposed to acute and chronic hypoxia. *Mol. Biol. Rep.* 39, 4009–4015. doi: 10.1007/s11033-011-1181-8

Rocca, Y. D., Fonticoli, L., Rajan, T. S., Trubiani, O., Caputi, S., Diomede, F., et al. (2022). Hypoxia: Molecular pathophysiological mechanisms in human diseases. *J. Physiol. Biochem.* 78, 739–752. doi: 10.1007/s13105-022-00912-6

Sampathkumar, N. K., Sundaram, V. K., Danthi, P. S., Barakat, R., Solomon, S., Mondal, M., et al. (2022). RNA-Seq is not required to determine stable reference genes for qPCR normalization. *PloS Comput. Biol.* 18 (2), e1009868. doi: 10.1371/journal.pcbi.1009868

San, L., Liu, B., Liu, B., Guo, H., Guo, L., Zhang, N., et al. (2021). Transcriptome analysis of gills provides insights into translation changes under hypoxic stress and reoxygenation in golden pompano, *trachinotus ovatus* (Linnaeus 1758). *Front. Mar. Sci.* 8. doi: 10.3389/fmars.2021.763622

Sarapultsev, A., Gusev, E., Komelkova, M., Utepova, I., Luo, S., and Hu, D. (2023). JAK-STAT signaling in inflammation and stress-related diseases: implications for therapeutic interventions. *Mol. BioMed.* 4, 40. doi: 10.1186/s43556-023-00151-1

Shaftoe, J. B., Manchester, E. A., and Gillis, T. E. (2023). Cardiac remodeling caused by cold acclimation is reversible with rewarming in zebrafish (*Danio rerio*). *Comp. Biochem. Physiol. Part A: Mol. Integr. Physiol.* 283, 111466. doi: 10.1016/j.cbpa.2023.111466

Sharma, D., Singh, M., and Rani, R. (2022). Role of LDH in tumor glycolysis: Regulation of LDHA by small molecules for cancer therapeutics. *Semin. Cancer Biol.* 87, 184–195. doi: 10.1016/j.semcancer.2022.11.007

Shati, A. A., Zaki, M. S. A., Alqahtani, Y. A., Haidara, M. A., Alshehri, M. A., Dawood, A. F., et al. (2022). Intermittent short-duration re-oxygenation attenuates cardiac changes in response to hypoxia: histological, ultrastructural and oxidant/antioxidant parameters. *Br. J. Biomed. Sci.* 79, 10150. doi: 10.3389/bjbs.2022.10150

Soe, K. K., Iqbal, T. H., Lim., A., Wang, W. X., Tsim, K. W. K., Takeuch, Y., et al. (2023). Reproductive characteristics of the hermaphroditic four-fnger threadfn, *Eleutheronema tetradactylum* (Shaw 1804), in tropical coastal waters. *BMC Zool.* 8, 22. doi: 10.1186/s40850-023-00181-w

Song, H., Mao, W., Duan, Z., Que, Q., Zhou, W., Chen, X., et al. (2020). Selection and validation of reference genes for measuring gene expression in *Toona ciliata* under different experimental conditions by quantitative real-time PCR analysis. *BMC Plant Biol.* 20, 450. doi: 10.1186/s12870-020-02670-3

Su, Z., Liu, Y., and Zhang, H. (2021). Adaptive cardiac metabolism under chronic hypoxia: mechanism and clinical implications. *Front. Cell Dev. Biol.* 9. doi: 10.3389/fcell.2021.625524

Sun, X., Tu, K., Li, L., Wu, B., Wu, L., Liu, Z., et al. (2021). Integrated transcriptome and metabolome analysis reveals molecular responses of the clams to acute hypoxia. *Mar. Environ. Res.* 168, 105317. doi: 10.1016/j.marenvres.2021.105317

Tang, D. D., and Gerlach, B. D. (2017). The roles and regulation of the actin cytoskeleton, intermediate filaments and microtubules in smooth muscle cell migration. *Respir. Res.* 18, 54. doi: 10.1186/s12931-017-0544-7

Terekhanova, N. V., Karpova, A., Liang, W., Strzalkowski, A., Chen, S., Li, Y., et al. (2023). Epigenetic regulation during cancer transitions across 11 tumour types. *Nature* 623, 432–441. doi: 10.1038/s41586-023-06682-5

Wallimann, T., Tokarska-Schlattner, M., and Schlattner, U. (2011). The creatine kinase system and pleiotropic effects of creatine. *Amino Acids* 40, 1271–1296. doi: 10.1007/s00726-011-0877-3

Wang, W., Huang, J., Zhang, J., Wang, Z., Li, H., Amenyogbe, E., et al. (2021). Effects of hypoxia stress on the intestinal microflora of juvenile of cobia (*Rachycentron canadum*). *Aquaculture* 536, 736419. doi: 10.1016/j.aquaculture.2021.736419

Wang, Z., Pu, D., Zheng, J., Li, P., Lü, H., Wei, X., et al. (2023). Hypoxia-induced physiological responses in fish: From organism to tissue to molecular levels. *Ecotoxicol. Environ. Saf.* 267, 115609. doi: 10.1016/j.ecoenv.2023.115609

Weir, E. K., and Olschewski, A. (2006). Role of ion channels in acute and chronic responses of the pulmonary vasculature to hypoxia. *Cardiovasc. Res.* 71, 630–641. doi: 10.1016/j.cardiores.2006.04.014

Westman, J., Walpole, G. F., Kasper, L., Xue, B. Y., Elshafee, O., Hube, B., et al. (2020). Lysosome fusion maintains phagosome integrity during fungal infection. *Cell Host Microbe* 28, 798–812.e6. doi: 10.1016/j.chom.2020.09.004

Wu, Y., Lai, X., Lin, B., Lin, Y., Yang, Y., Zhang, M., et al. (2023). Transcriptome and hypoxia-responsive gene expression analyses reveal the physiological reaction to acute hypoxia and reoxygenation in *Epinephelus coioides*. *Aquacult. Rep.* 31, 101655. doi: 10.1016/j.aqrep.2023.101655

Xie, Rt., Amenyogbe, E., Wang, W.-Z., Guo, Z.-X., Chen, G., and Huang, J.-S. (2021). Cloning and expression analysis of hypoxia-related gene HO in cobia. *Aquacult. Int.* 29, 75–89. doi: 10.1007/s10499-020-00611-3

Xie, J., Luo, S., and Liu, G. (2024). Research progress on PCK1 regulating cell aging through energy metabolism. *Chem. Life* 44, 102–109.

Xuan, Z., and Wang, W. (2023). Chemometric analysis of fish fin ray multi-elemental signatures with differentiation of wild and farmed fourfinger threadfin fish. *J. Food Composition Anal.* 123, 105597. doi: 10.1016/j.jfca.2023.105597

Ye, J., Zheng, L., Chen, Z., Wang, Q., Liao, X., Wang, X., et al. (2024). Serum α-hydroxybutyrate dehydrogenase as a biomarker for predicting survival outcomes in patients with UTUC after radical nephroureterectomy. *BMC Urol.* 24, 62. doi: 10.1186/s12894-024-01439-2

Yfantis, A., Mylonis, I., Chachami, G., Nikolaidis, M., Amoutzias, G. D., Paraskeva, E., et al. (2023). Transcriptional response to hypoxia: the role of HIF-1-associated co-regulators. *Cells* 12 (5), 798. doi: 10.3390/cells12050798

Yohana, W. Y., Nasution, T. I., Wahyuningsih, H., Matondang, A. A., and Margolang, A. R. (2024). Evaluation of dissolved oxygen concentration in different circulation systems on water quality in fish pond. *J. Appl. Geospatial Inf.* 8, 71–77. doi: 10.30871/jagi.v8i1.7820

Yu, S., Meng, S., Xiang, M., and Ma, H. (2021). Phosphoenolpyruvate carboxykinase in cell metabolism: Roles and mechanisms beyond gluconeogenesis. *Mol. Metab.* 53, 101257. doi: 10.1016/j.molmet.2021.101257

Zhang, J.-D., Li, H.-J., Amenyogbe, E., Wang, W.-Z., Huang, J.-S., and Chen, G. (2021). Cloning of Mn-SOD gene and its mRNA expression difference and antioxidant enzyme activities under hypoxia stress of cobia *Rachycentron canadum. Mol. Biol. Rep.* 48 (10), 6897-6909. doi: 10.1007/s11033-021-06692-4

Zhang, H., Li, R., Wang, Y., Zhou, J., Xu, H., Gou, M., et al. (2023a). Transcriptomic Analysis of *Takifugu obscurus* Gills under Acute Hypoxic Stress. *Animals: Open Access J. From MDPI* 13 (10), 1572. doi: 10.3390/ani13101572

Zhang, Y., Zhang, D., Tian, Y., Mao, J., Liu, Y., and Hao, Z. (2023b). Transcriptome analysis of gill tissues from *neptunea cumingii* in different seasons. *Fishes* 8, 549. doi: 10.3390/fishes8110549

Zhao, Y., Xiong, W., Li, C., Zhao, R., Lu, H., Song, S., et al. (2023). Hypoxia-induced signaling in the cardiovascular system: Pathogenesis and therapeutic targets. *Signal Transduction Targeted Ther.* 8, 1–42. doi: 10.1038/s41392-023-01652-9